Astron. Astrophys. 347, 594–616 (1999)

ASTRONOMY AND ASTROPHYSICS

Mineral formation in stellar winds

I. Condensation sequence of silicate and iron grains in stationary oxygen rich outflows

H.-P. Gail[1] **and E. Sedlmayr**[2]

[1] Institut für Theoretische Astrophysik, Universität Heidelberg, Tiergartenstrasse 15, D-69121 Heidelberg, Germany (gail@ita.uni-heidelberg.de)
[2] Institut für Astronomie und Astrophysik, Technische Universität Berlin, Hardenbergstrasse 36, D-10623 Berlin, Germany (sedlmayr@physik.tu-berlin.de)

Received 10 August 1998 / Accepted 23 March 1999

Abstract. This paper considers the growth of circumstellar dust grains formed from the elements silicon, magnesium, and iron. The stability of olivine ($Mg_{2x}Fe_{2(1-x)}SiO_4$), quartz (SiO_2), iron, and periclase (MgO) dust in a circumstellar environment is discussed. The role of exchange of Fe^{2+} and Mg^{2+} cations, solid diffusion of Fe^{2+} cations within the SiO_4 matrix of the silicate lattice, and annealing of an initially amorphous lattice structure during olivine growth is considered. The complete set of equations describing the vapourisation and growth of a mixture of olivine, quartz, iron, and periclase grains, including the internal diffusion and the surface exchange processes, is derived. These equations are solved for a simplified model of a stellar wind for the case of an M star. The calculation shows that for M stars the dust in the circumstellar shell is a multicomponent mixture dominated by olivine and iron grains. Olivine grains likely show variations of their magnesium and iron content between the core and the surface. Some periclase and a tiny fraction of quartz also are formed in the outflow.

Key words: stars: circumstellar matter – stars: mass-loss – stars: AGB and post-AGB

1. Introduction

During the late stages of stellar evolution, on the asymptotic giant branch (AGB), stars with initial masses on the main sequence in the range $1\,M_\odot \lesssim M \lesssim 8\,M_\odot$ loose a significant fraction of their mass during a short phase of an intense mass-loss. In this phase they are enshrouded by an optically thick dust shell, in which solids condense from the gas phase as tiny dust grains. Most of the observed objects have an oxygen rich element composition and show in the infrared spectral region in their emission two broad emission features at roughly 9.7 μm and 18 μm. These are generally believed to be associated with vibrational modes of the fundamental SiO_4 tetrahedron in silicate condensates of a largely disordered lattice structure. A somewhat smaller fraction of the objects has a carbon rich element mixture; they are not considered in this paper.

Besides these main features some less pronounced features have been detected. A broad feature around 13 μm found in a number of objects usually is ascribed to corundum dust grains (Vardya et al. 1986, Onaka et al. 1989, Little-Marenin & Little 1990, Stencel et al. 1990, Begemann et al. 1997). Some other features observed between 10 μm and 19 μm are ascribed to metal oxides and/or crystalline silicates (Goebel et al. 1989, 1994)

Recent observations in the far infrared spectral region with the ISO satellite revealed the existence of a series of dust features in the wavelength region between 30 and 44 μm. These are tentatively identified with features of crystalline olivine ($Mg_{2x}Fe_{2(1-x)}SiO_4$) and pyroxene ($Mg_xFe_{1-x}SiO_3$) (Waters et al. 1996). These observations show that the dust formation process in oxygen-rich circumstellar shells results in the formation a variety of dust components with quite different mineral compositions and lattice structures ranging from being completely disordered amorphous condensates to crystalline materials.

From a theoretical point of view the formation and growth of such grains is still a widely unsolved problem. In order to shed light on this unsatisfactory situation, as a first order approximation, in this paper we refer to the highly simplified picture of a stationary stellar outflow. For this cooling flow we (i) discuss the stability conditions of the relevant condensates and (ii) investigate heterogeneous, non-equilibrium grain growth by adopting suitable seed nuclei and a reasonable chemical gas phase composition, typical for the shells of M giants. From the results we expect a better insight into the complex grain formation processes taking place, providing a safer physical basis for more realistic future descriptions, e.g. for modelling dust formation in Miras and LPV's.

We concentrate on the formation of dust from the most abundant elements forming refractory compounds: Mg, Si, and Fe. These elements, together with oxygen, form the main dust components responsible for most of the dust opacity and the emis-

Send offprint requests to: H.-P. Gail

sion of infrared radiation. Less abundant dust species like corundum are not discussed in this paper. Also we do not consider the problem of nucleation of dust grains but simply assume that the main dust components grow on seed nuclei, which are formed at a temperature somewhat above the stability limits of the main dust components. The problem of nucleation is discussed in Gail & Sedlmayr (1998b).

The plan of this paper is as follows: in Sect. 2 we discuss the stability limits of the possible condensates formed from Mg, Si, and Fe. In Sect. 3 we discuss the basic principles of grain growth and vapourisation for the essential dust components, including the exchange process of Fe^{2+} and Mg^{2+} cations for olivine dust. In Sect. 4 we consider cation diffusion in olivine and annealing processes. Sect. 5 contains results of a preliminary model calculation for the formation of a multicomponent dust mixture in the wind of M stars. Sect. 6 contains some concluding remarks and an appendix briefly present our method for solving numerically the coupled problem of grain growth and cation diffusion within the grains.

2. Equilibrium chemistry of the Si-Mg-Fe complex

If one tries to calculate the condensation and growth of dust in circumstellar shells one of the most important questions is the temperature and pressure where some specific solid compound starts to condense from the gas phase in a cooling gas. The onset of condensation depends critically on the question whether there exist already surfaces, on which the special compound can be precipitated or not. If no surfaces exist, condensation first requires the formation of some kind of seed nuclei from the gas phase which is a process quite different from the growth of a condensate and is a difficult problem of its own which is not considered in this work. In the opposite case, if surfaces already exist, condensates usually can easily grow on these surfaces once the condensed phase becomes thermodynamically stable, which means that in a thermodynamic equilibrium state part (or all) of the previously gaseous material reacts to form a solid compound.

Condensation of dust in circumstellar shells is a process which operates under conditions far from thermodynamic equilibrium. Nevertheless it is instructive to start the discussion with some considerations based on equilibrium thermodynamics. Such discussions have a long history, starting with the note of Gilman (1969). A brief discussion of the main facts with respect to equilibrium condensation under circumstellar conditions was given by Salpeter (1977). Equilibrium condensation also has extensively been discussed in the context of the chemistry of the Solar Nebula (e.g. Grossman 1972, Lattimer et al. 1978, Saxena & Ericksson 1986, Sharp & Huebner 1990). More recently, condensation of circumstellar dust has been discussed by Gail & Sedlmayr (1998a, 1998b). Such calculations show that for pressure-temperature conditions encountered in the condensation zone of circumstellar dust shells ($T \approx 1\,000$ K, $P \approx 10^{-4}$ dyn·cm^{-2}) the most stable condensate formed from the abundant elements Si, Fe and Mg is forsterite with composition Mg_2SiO_4, followed by enstatite with composition $MgSiO_3$ and metallic iron. All these compounds have their stability limits under equilibrium conditions in the temperature region between ≈ 800 K and $\approx 1\,100$ K, depending on the specific compound and the gas pressure. At much lower temperature some other compounds of these elements (e.g. FeS, Fe_3O_4) may become more stable (cf. Saxena & Ericsson 1986) but it is unlikely that these can be formed in stellar winds (Gail & Sedlmayr 1998a). In the following we give a modified and extended version of the discussion of equilibrium condensation of compounds of silicon, magnesium, and iron of Gail (1998a) and Gail & Sedlmayr (1999) which fits to the requirements of our later non-equilibrium calculations.

2.1. Stability of magnesium-iron silicates

The most stable condensate formed from the abundant elements O, Si, Mg, and Fe is the magnesium-iron silicate $Mg_{2x}Fe_{2(1-x)}SiO_4$ with $x \in [0,1]$. The end members of this continuous series of compounds are forsterite with $x = 1$ and fayalite with $x = 0$. The mixed compound with $0 < x < 1$ is called olivine. The olivine can be considered as an ideal solution of fayalite in forsterite (cf. Saxena & Ericksson 1986). Pure forsterite is stable up to the highest temperature while pure fayalite has a much lower stability limit.

If we consider the stability of these species, we have to consider that circumstellar dust grains are embedded in a carrier gas which is dominated by hydrogen. There emerge two possibilities:

- The microscopic reactions responsible for the destruction of the silicate dust are not affected by the presence of hydrogen. In this case olivine decomposes as if it is vapourised in vacuo.
- The hydrogen reacts with the SiO_4 groups at the surface and reduces the silicon to free SiO, Mg, and Fe molecules and water vapour. In this case the silicate is disintegrated by a process which we may call chemisputtering.

We consider both processes in turn.

2.1.1. Free evaporation

The pure *thermal decomposition* can be considered as a chemical reaction of the type

$$\mathrm{Mg_{2x}Fe_{2(1-x)}SiO_4(s)} \longrightarrow 2x\mathrm{Mg} + 2(1-x)\mathrm{Fe} + \mathrm{SiO} + 3\mathrm{O}$$

in which the solid disintegrates into free molecules. The molecule SiO and the free atoms Mg, Fe, and O are the most abundant gas phase species that exist in chemical equilibrium at temperatures $T \gtrsim 1\,000$ K. However, some other molecules can also be formed, especially O_2 is also very abundant. The true vapour in chemical equilibrium is a mixture of several species which is dominated by the four species SiO, O_2, Mg, and Fe. In order to calculate the partial pressures of the gas phase species we have to consider the chemical equilibrium state between

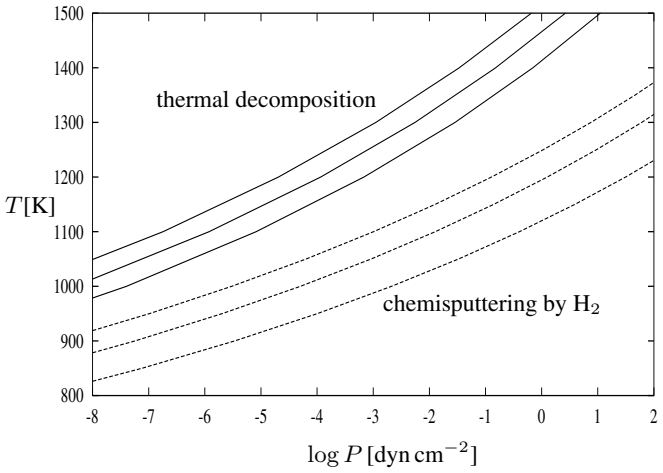

Fig. 1. Stability limits of olivine with respect to pure thermal decomposition (full lines) and chemisputtering (dashed lines) for three different compositions: $x = 1$ (upper lines) corresponding to pure forsterite, $x = 0.5$ (middle lines), an iron rich olivine, and $x = 0$ (bottom lines) corresponding to pure fayalite.

olivine and its decomposition products. The two extreme cases $x = 1$ and $x = 0$ have been considered in Duschl et al. (1996). We have calculated the decomposition equilibrium for olivine with $0 \le x \le 1$ analogously to the method described in their appendix and determined the vapour pressure $p_{v,\mathrm{SiO}}$ of SiO molecules over solid olivine.

In doing this we assumed olivine to form an ideal solution of forsterite (Mg_2SiO_4) and fayalite (Fe_2SiO_4). Experimentally it is found that this assumption is correct; deviations from ideality are very small (cf. Saxena & Ericksson 1986). The free enthalpy of formation of one mole of olivine then is given by

$$\Delta G(\mathrm{ol}) = x\Delta G(\mathrm{for}) + (1-x)\Delta G(\mathrm{fa}) + \Delta G_{\mathrm{mix}} \tag{1}$$

where $\Delta G(\mathrm{fo})$ and $\Delta G(\mathrm{fa})$ are the free energies of formation from the free atoms of one mole of olivine and fayalite, respectively. Here and in the following we abbreviate the mineral names olivine, forsterite, and fayalite by "ol", "fo", and "fa", respectively. The entropy of mixing is

$$\Delta G_{\mathrm{mix}} = 2RT\,(x\ln x + (1-x)\ln(1-x)) \tag{2}$$

because the Mg^{++} and Fe^{++} ions are distributed over two moles of cation sites. Thermochemical data for molecules and solids are taken here and in all our following calculations from Sharp & Huebner (1990), if not explicitly stated otherwise.

Let f_{ol} denote the fraction of the silicon condensed in olivine. In the gas phase at temperatures $T \gtrsim 1\,000\,\mathrm{K}$ only the SiO molecule is abundant. Other silicon compounds and free Si atoms have completely negligible abundances. The partial pressure p_{SiO} of SiO molecules in the gas phase then is

$$p_{\mathrm{SiO}} = (1-f_{\mathrm{ol}})\epsilon_{\mathrm{Si}} P_{\mathrm{H}}\,. \tag{3}$$

Here P_{H} denotes the fictitious pressure of all hydrogen nuclei. Under pressure-temperature conditions where dust condenses in circumstellar dust shells ($P \approx 10^{-4}\,\mathrm{dyn\,cm^{-2}}$, $T \approx 1\,000\,\mathrm{K}$) the hydrogen is completely associated to H_2. Then we have

$$P_{\mathrm{H}} = \frac{2}{1+2\epsilon_{\mathrm{He}}}\,P\,. \tag{4}$$

In equilibrium between olivine and the gas phase the partial pressure in the gas phase p_{SiO} equals the vapour pressure $p_{v,\mathrm{SiO}}$ of SiO over olivine. Then we have

$$P = \frac{1+2\epsilon_{\mathrm{He}}}{2(1-f_{\mathrm{ol}})\epsilon_{\mathrm{Si}}}\,p_{v,\mathrm{SiO}}\,. \tag{5}$$

The stability limit of olivine is defined by $f_{\mathrm{ol}} = 0$. This defines a limit curve in the P-T-plane above and to the left of which no olivine exist while below and to the right of this limit curve part or all of the silicon is condensed into olivine. Some limit curves of stability for different compositions of olivine (different values of x) are shown in Fig. 1 as full lines.

If the silicate disintegrates by pure thermal decomposition despite the presence of a lot of hydrogen, then the decomposition process operates under conditions far from chemical equilibrium between the gas phase and the solid since the decomposition products O and O_2 have negligible abundances in a hydrogen rich environment. After being liberated by thermal decomposition they immediately react in the gas phase with H_2 to form H_2O. The chemical composition of the gas phase with respect to the abundance of species produced by vapourisation, thus, is different from their abundance in the vapour. The solid and the gas phase are not in chemical equilibrium in this case.

2.1.2. Chemisputtering

Chemical equilibrium between solid olivine and a hydrogen rich environment requires that disintegration occurs according to the following chemical net reaction

$$\mathrm{Mg_{2x}Fe_{2(1-x)}SiO_4(s)} + 3\mathrm{H_2} \longrightarrow 2x\mathrm{Mg} + 2(1-x)\mathrm{Fe} + \mathrm{SiO} + 3\mathrm{H_2O} \tag{6}$$

since the dominating gas phase species of the elements Si, Fe, and Mg are not changed by the presence of hydrogen, but the oxygen forms water vapour. In chemical equilibrium the partial pressures of the gas phase species have to satisfy the law of mass action

$$\frac{p_{\mathrm{Mg}}^{2x}\,p_{\mathrm{Fe}}^{2(1-x)}\,p_{\mathrm{SiO}}\,p_{\mathrm{H_2O}}^{3}}{p_{\mathrm{H_2}}^{3}} = \mathrm{e}^{-\Delta G/RT} = K_p^{-1}(\mathrm{ol}) \tag{7}$$

where ΔG is the change of free enthalpy in reaction (6). This is given by

$$\Delta G = 2x\Delta G(\mathrm{Mg}) + 2(1-x)\Delta G(\mathrm{Fe}) + \Delta G(\mathrm{SiO}) + 3\Delta G(\mathrm{H_2O}) - \Delta G(\mathrm{ol}) - 3\Delta G(\mathrm{H_2}) \tag{8}$$

where $\Delta G(xy)$ denotes the free enthalpy of formation of xy from the free atoms.

Since magnesium and iron are present in the gas phase as free atoms their partial pressures are $p_{\mathrm{Mg}} = (\epsilon_{\mathrm{Mg}} - 2x f_{\mathrm{ol}}\epsilon_{\mathrm{Si}})P_{\mathrm{H}}$ and $p_{\mathrm{Fe}} = (\epsilon_{\mathrm{Fe}} - 2(1-x)f_{\mathrm{ol}}\epsilon_{\mathrm{Si}})P_{\mathrm{H}}$. Since oxygen bearing

species from the gas phase other than CO, SiO, and H_2O have negligible abundances, the partial pressure of H_2O is $p_{H_2O} = (\epsilon_O - \epsilon_C - (1+3f_{ol})\epsilon_{Si})P_H$ if we assume that no other oxygen bearing solid than olivine exists. The partial pressure of H_2 is $p_{H_2} = \frac{1}{2}P_H$. It follows from (7)

$$P^3 = \frac{(1+2\epsilon_{He})^3}{(\epsilon_{Mg} - 2xf_{ol}\epsilon_{Si})^{2x}\ (\epsilon_{Fe} - 2(1-x)f_{ol}\epsilon_{Si})^{2(1-x)}} \frac{1}{2^6\ (1-f_{ol})\,\epsilon_{Si}\ (\epsilon_O - \epsilon_C - (1+3f_{ol})\epsilon_{Si})^3\ K_p(ol)}\,. \quad (9)$$

The curve in the P-T-plane defined by $f_{ol} = 0$ and given x describes the stability limit of olivine in chemical equilibrium with the gas phase. Above and to the left of this line no olivine exists in a chemical equilibrium state. Below and to the right of the limit line part of the silicon is bound in solid olivine. Some limit curves of stability for different compositions of olivine (different values of x) are shown in Fig. 1 as dashed lines.

The stability limit of olivine in chemical equilibrium occurs $100 \ldots 200$ K below the stability limit for thermal decomposition. Thus, the true stability limit depends critically on the question whether there exist chemical surface reactions between olivine and the hydrogen molecules which disintegrate the solid. The recent laboratory experiments of Nagahara & Ozawa (1994, 1996) on forsterite vapourisation in the presence of H_2 have shown, that such reactions really do occur. They found in their experiment conducted at 1 973 K and H_2 pressures between 10^{-3} and $3\,10^1$ dyn cm^{-2} a linear dependence of the vapourisation rate on the H_2 pressure in the high pressure region and a pressure independent vapourisation rate for their lowest pressures. They interpreted their experimentally determined decomposition rates as being a superposition of free vapourisation, which dominates for very low H_2 pressures, and chemisputtering, which dominates at high pressures. The fit to their experimentally determined vapourisation rate is given as (Nagahara & Ozawa 1994)

$$J^{vap} = 8.0\,10^{-7} + 2.7\,10^{-7}\,p_{H_2}\ [\mathrm{gramm \cdot cm^{-2} \cdot s^{-1}}]\,. \quad (10)$$

The free vapourisation rate is consistent with the experimentally determined rate of vapourisation in vacuo of forsterite, as determined for instance by Hashimoto (1990).

In the detailed analysis of their experiment Nagahara & Ozawa (1996) compared their measured chemisputtering rate with the expression

$$J^{dep} = \alpha \sum_i \frac{p_i}{\sqrt{2\pi m_i kT}} \quad (11)$$

for the theoretical deposition rate of Si bearing species i from the gas phase at the surface of forsterite if the forsterite is in kinetic equilibrium with the gas phase with respect to chemisputtering and growth. They calculated J^{dep} for a chemical equilibrium gas phase composition at the H_2 pressures of the experiment and derived a value for the sticking coefficient α of the order of 0.1. Since SiO has a much bigger abundance than all other Si bearing molecules in the gas phase, J^{dep} is determined essentially by

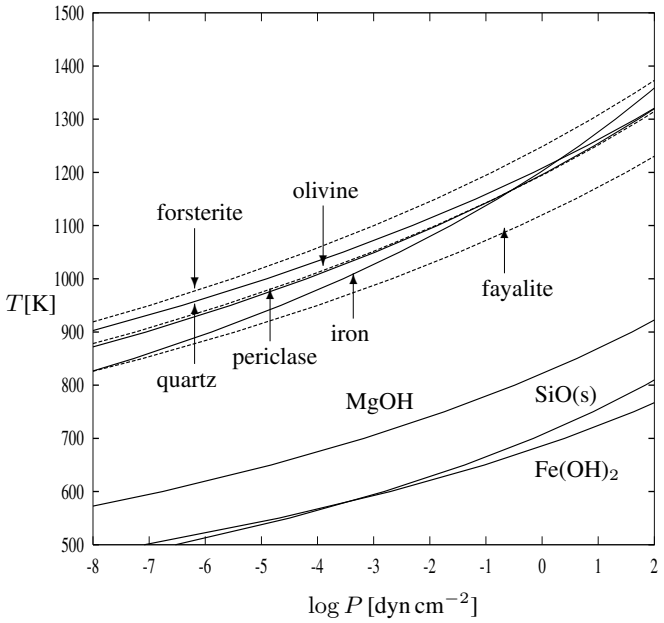

Fig. 2. Stability limits of some solids and molecules. The dashed lines show the stability limits for Olivine $Mg_{2x}Fe_{2(1-x)}SiO_4$ for three different compositions: $x = 1$ (top), i.e. pure forsterite, $x = 0.5$ (middle), an iron rich olivine, and $x = 0$ (bottom), i.e. pure fayalite.

SiO. This also means that the deposition of SiO at the surface is the rate determining step for the growth of forsterite.

The experimental finding that chemisputtering occurs if forsterite is embedded in a hot H_2 gas means that the stability limit (9) is the relevant one for condensation or vapourisation in circumstellar dust shells and not that of thermal decomposition considered in the previous section.

A different iron-magnesium silicate which may condense in a circumstellar dust shell is orthopyroxene with composition $Mg_xFe_{1-x}SiO_3$. This material is not considered in this paper for reasons which are explained below.

2.2. Condensation of silicon oxides

The silicon forms the two solid oxides SiO and quartz (SiO_2) which may be formed from the SiO molecules in the gas phase. In calculations of the equilibrium composition of a solid-gas mixture with standard cosmic element composition both solids are not found as condensed species. This is because the silicon is completely consumed by the formation of the much more stable olivine and pyroxene and some minor compounds (e.g. Lattimer et al. 1978, Sharp & Huebner 1990). In spite of this, in a circumstellar shell these oxides may be formed due to rapid cooling of the outflow and slow growth of solids which means that much of the gas phase components are not yet condensed at temperatures where they would completely be consumed by formation of solids under equilibrium conditions. At temperatures around 1 000 K the silicon not yet condensed in solids is present as the molecule SiO. Once the gas temperature of the outflow drops below the stability limit of quartz or solid SiO these substances may start to condense as separate solid species. If cooling is suf-

ficient rapid such that the increase of the supersaturation ratio of SiO due to cooling always exceeds the reduction of the supersaturation ration due to SiO consumption by particle growth for all solid silicate compounds present in the outflow, all these species continue to grow from the gas phase[1], until the gas is so much diluted that all growth processes are stalled.

The quartz can be formed from the gas phase by the reaction

$$\mathrm{SiO} \;+\; \mathrm{H_2O} \;\longrightarrow\; \mathrm{SiO_2(s)} \;+\; \mathrm{H_2}\,.$$

In chemical equilibrium between the gas phase and the condensate we have

$$\frac{p_{\mathrm{H_2}}}{p_{\mathrm{SiO}}\,p_{\mathrm{H_2O}}} = \mathrm{e}^{-\Delta G/RT} = K_p(\mathrm{qu})\,. \tag{12}$$

Here we abbreviate with "qu" the mineral name quartz. We denote by f_{qu} the fraction of the Si condensed into quartz. The partial pressure of SiO in the gas phase then is given by $p_{\mathrm{SiO}} = (1 - f_{\mathrm{qu}} - f_{\mathrm{ol}} - f_{\mathrm{py}})\epsilon_{\mathrm{Si}}P_{\mathrm{H}}$, assuming that part of the silicon is already condensed into olivine and pyroxene, and the partial pressure of water vapour is $p_{\mathrm{H_2O}} = (\epsilon_{\mathrm{O}} - \epsilon_{\mathrm{C}} - (1 + f_{\mathrm{qu}} + 2f_{\mathrm{py}} + 3f_{\mathrm{ol}})\epsilon_{\mathrm{Si}})P_{\mathrm{H}}$. It follows from the law of mass action

$$P \;=\; \frac{1 + 2\epsilon_{\mathrm{He}}}{4\,(1 - f_{\mathrm{qu}} - f_{\mathrm{ol}} - f_{\mathrm{py}})\,\epsilon_{\mathrm{Si}}} \frac{1}{(\epsilon_{\mathrm{O}} - \epsilon_{\mathrm{C}} - (1 + f_{\mathrm{qu}} + 2f_{\mathrm{py}} + 3f_{\mathrm{ol}})\epsilon_{\mathrm{Si}})\,K_p(\mathrm{qu})}\,. \tag{13}$$

The curve with $f_{\mathrm{qu}} = 0$ is the limit curve below and to the right of which quartz becomes thermodynamically stable. This limit curve (assuming $f_{\mathrm{ol}} = f_{\mathrm{py}} = 0$) is shown in Fig. 2. If some fraction of the silicon is already condensed into olivine or pyroxene, it is shifted to a somewhat higher pressure for given T.

Obviously, quartz becomes thermodynamically stable at a temperature only slightly below the stability limits of enstatite but much above the stability limit of fayalite. It depends, thus, on the iron content of the olivine during the very first growth phase, which one of the two condensates, olivine or quartz, appears first. In chemical equilibrium the olivine would be very iron poor, $x \gtrsim 0.99$, as is shown in Gail & Sedlmayr (1998a). Then olivine condenses first and at an approximately 20 K lower temperature quartz becomes stable and starts to condense. If, however, the composition of olivine during the initial growth process is more iron rich than in chemical equilibrium, as it might be for kinetical reasons, then quartz is the first silicate component which starts to condense and olivine appears at some lower temperature. This problem is treated in detail in Sect. 3.4.

Next we consider the possible condensation of silicon monoxide. We take its vapour pressure from Nuth & Donn (1982b)

$$p_{v,\mathrm{SiO}} = \mathrm{e}^{12.81 - 25700/T}\;[\mathrm{atm}]\,. \tag{14}$$

[1] In a system evolving into equilibrium the reduction of the gas phase abundance of SiO by particle growth ultimately reduces the partial pressure of SiO to a level where the gas phase for the least stable species becomes subsaturated. This species then starts to vapourise in favour of growth of the more stable species until finally only the most stable species survive.

The gas phase pressure of SiO at the stability limit of SiO(s), if no other silicate would be condensed, is $p_{\mathrm{SiO}} = \epsilon_{\mathrm{Si}}P_{\mathrm{H}}$. We obtain the following limit curve for the condensation of SiO

$$P = \frac{(1 + 2\epsilon_{\mathrm{He}})p_{v,\mathrm{SiO}}}{2\epsilon_{\mathrm{Si}}} \tag{15}$$

which is shown in Fig. 2. Solid silicon monoxide becomes stable only at very low temperatures ($T \lesssim 500$ K) when the dust growth process in the stellar wind is nearly completed. Thus, SiO does not condense as a separate dust species and needs not to be considered further.

2.3. Condensation of periclase

Magnesium forms the very stable oxide periclase (MgO). This, again, is not found to be a condensate in equilibrium calculations for condensates in a Solar System element mixture (e.g. Lattimer et al. 1978, Sharp & Huebner 1990) since Mg is completely bound in compounds with Si and Al, which are even more stable than periclase. In a circumstellar shell it may, in spite of this, be formed due to rapid cooling of the outflow and slow growth of solids which means that much of the gas phase components are not yet condensed at temperatures where they would completely be consumed by formation of solids under equilibrium conditions. Since at temperatures around 1 000 K the Mg not yet condensed in solids is present as the free atom, periclase may be formed in the reaction

$$\mathrm{Mg} \;+\; \mathrm{H_2O} \;\longrightarrow\; \mathrm{MgO(s)} \;+\; \mathrm{H_2}$$

once the solid becomes thermodynamically stable. This reaction may for instance occur at the surface of growing magnesium silicates in competition with the growth of the substrate. In chemical equilibrium between periclase and the gas phase we would have

$$\frac{p_{\mathrm{H_2}}}{p_{\mathrm{Mg}}\,p_{\mathrm{H_2O}}} = \mathrm{e}^{-\Delta G/RT} = K_p(\mathrm{pe})\,. \tag{16}$$

Here we abbreviate with "pe" the mineral name periclase. We denote by f_{pe} the fraction of the Mg condensed into periclase. The partial pressure of Mg in the gas phase then is given by $p_{\mathrm{Mg}} = ((1 - f_{\mathrm{pe}})\epsilon_{\mathrm{Mg}} - (2x_{\mathrm{ol}}f_{\mathrm{ol}} + x_{\mathrm{py}}f_{\mathrm{py}})\epsilon_{\mathrm{Si}})P_{\mathrm{H}}$ and that of water vapour by $p_{\mathrm{H_2O}} = (\epsilon_{\mathrm{O}} - \epsilon_{\mathrm{C}} - (1 + f_{\mathrm{qu}} + 2f_{\mathrm{py}} + 3f_{\mathrm{ol}})\epsilon_{\mathrm{Si}})P_{\mathrm{H}}$. It follows from the law of mass action

$$P = \frac{1 + 2\epsilon_{\mathrm{He}}}{4\,K_p(\mathrm{pe})}\,((1 - f_{\mathrm{pe}})\epsilon_{\mathrm{Mg}} - (2x_{\mathrm{ol}}f_{\mathrm{ol}} + x_{\mathrm{py}}f_{\mathrm{py}})\epsilon_{\mathrm{Si}})^{-1} \\ (\epsilon_{\mathrm{O}} - \epsilon_{\mathrm{C}} - (1 + f_{\mathrm{qu}} + 2f_{\mathrm{py}} + 3f_{\mathrm{ol}})\epsilon_{\mathrm{Si}} - f_{\mathrm{pe}}\epsilon_{\mathrm{Mg}})^{-1}\,. \tag{17}$$

The curve in the P-T-plane with $f_{\mathrm{pe}} = 0$ defines the limit curve below and to the right of which periclase becomes stable. This limit curve (assuming $f_{\mathrm{ol}} = f_{\mathrm{py}} = f_{\mathrm{qu}} = 0$) is shown in Fig. 2. If some fraction of the silicon is already condensed into olivine, pyroxene, or quartz, it is shifted to a somewhat higher pressure for given T. Periclase obviously becomes stable at a temperature only slightly below the stability limits of the silicon compounds and may well be formed in a non-equilibrium

condensation process. It is, thus, to be considered as being a possible condensate in circumstellar dust shells of M stars.

Calculations of the chemical equilibrium composition of the gas phase show that at sufficiently low temperature MgOH becomes the dominating molecular compound of Mg. Since the dominating oxygen bearing species in the gas phase is H_2O the chemical reaction for its formation is

$$2\mathrm{Mg} \;+\; 2\mathrm{H_2O} \;\longrightarrow\; 2\mathrm{MgOH} \;+\; \mathrm{H_2}\,.$$

In chemical equilibrium we have

$$\frac{p_{\mathrm{MgOH}}^2\, p_{\mathrm{H_2}}}{p_{\mathrm{Mg}}^2\, p_{\mathrm{H_2O}}^2} = \mathrm{e}^{-\Delta G/RT} = K_p(\mathrm{MgOH})\,. \tag{18}$$

The limit curve in the P-T-plane where one half of the Mg available in the gas phase is converted into MgOH is obtained by letting $p_{\mathrm{Mg}} = p_{\mathrm{MgOH}}$ in (24). The partial pressure of H_2O in the gas phase then is

$$\begin{aligned} p_{\mathrm{H_2O}} \;=\; & \big[\epsilon_{\mathrm{O}} - \epsilon_{\mathrm{C}} - (1 + f_{\mathrm{qu}} + 2f_{\mathrm{py}} + 3f_{\mathrm{ol}})\epsilon_{\mathrm{Si}} \\ & -\tfrac{1}{2}[(1 - f_{\mathrm{pe}})\epsilon_{\mathrm{Mg}} + (2x_{\mathrm{ol}} f_{\mathrm{ol}} + x_{\mathrm{py}} f_{\mathrm{py}})\epsilon_{\mathrm{Si}}]\big]\, P_{\mathrm{H}}\,. \end{aligned} \tag{19}$$

It follows

$$\begin{aligned} P \;=\; & \frac{1 + 2\epsilon_{\mathrm{He}}}{4K_p(\mathrm{MgOH})}\Big(\epsilon_{\mathrm{O}} - \epsilon_{\mathrm{C}} - \Big[1 + f_{\mathrm{qu}} + \frac{3 + x_{\mathrm{py}}}{2} f_{\mathrm{py}} \\ & +(2 + x_{\mathrm{ol}}) f_{\mathrm{ol}}\Big]\epsilon_{\mathrm{Si}} - \frac{1 - f_{\mathrm{pe}}}{2}\epsilon_{\mathrm{Mg}}\Big)^{-2}\,. \end{aligned} \tag{20}$$

This limit curve is shown in Fig. 2. The magnesium hydroxide molecule occurs at such a low temperature that periclase in any case condenses (if it does) before MgOH consumes significant fractions of the gas phase Mg. It needs not to be considered further in the context of condensation.

2.4. Condensation of iron

Iron is found to be a condensate in equilibrium calculations for solid-gas mixtures with Solar System element mixture (e.g. Lattimer et al. 1978, Sharp & Huebner 1990). At temperatures of the order of 1 000 K or above and pressures typical for the circumstellar condensation zone iron is present in the gas phase as the free atom. Its partial pressure in the gas phase is

$$\begin{aligned} p_{\mathrm{Fe}} \;=\; & ((1 - f_{\mathrm{ir}})\epsilon_{\mathrm{Fe}} - 2(1 - x_{\mathrm{ol}}) f_{\mathrm{ol}}\epsilon_{\mathrm{Si}} \\ & -(1 - x_{\mathrm{py}}) f_{\mathrm{py}}\epsilon_{\mathrm{Si}})\, P_{\mathrm{H}}\,. \end{aligned} \tag{21}$$

where f_{ir} denotes the fraction of the element Fe condensed into solid iron. We have considered that part of the Fe may be condensed into olivine and pyroxene. The condensation of solid iron from the gas phase corresponds to the simple chemical reaction

$$\mathrm{Fe} \;\longrightarrow\; \mathrm{Fe(s)}\,.$$

Under chemical equilibrium conditions between the gas phase and condensed solid iron we have

$$\frac{1}{p_{\mathrm{ir}}} = \mathrm{e}^{-\Delta G/RT} = K_p(\mathrm{ir})\,. \tag{22}$$

We abbreviated with "ir" the name of the metal iron. p_{ir} is the vapour pressure of iron. Then we have

$$P = \frac{(1 + 2\epsilon_{\mathrm{He}})K_p(\mathrm{ir})}{2\,((1 - f_{\mathrm{ir}})\epsilon_{\mathrm{Fe}} - 2(1 - x_{\mathrm{ol}}) f_{\mathrm{ol}}\epsilon_{\mathrm{Si}} - (1 - x_{\mathrm{py}}) f_{\mathrm{py}}\epsilon_{\mathrm{Si}})} \tag{23}$$

For $f_{\mathrm{ir}} = 0$ this defines the stability limit of solid iron in the P-T plane. This limit curve (assuming $f_{\mathrm{ol}} = f_{\mathrm{py}} = 0$) is shown in Fig. 2. If some fraction of the iron is already condensed into olivine or pyroxene, it is shifted to a somewhat higher pressure for given T.

The iron starts to condenses at a temperature well below the stability limits of forsterite, quartz, and periclase. Only for very iron rich olivines the condensation temperature of olivine may fall below the condensation temperature of solid iron. In any case, iron is not the first condensate starting to grow on the seed nuclei.

Calculations of the chemical equilibrium composition of the gas phase show that at sufficiently low temperature $Fe(OH)_2$ becomes the dominating molecular compound of Fe. Since the dominating oxygen bearing species in the gas phase is H_2O the required chemical reaction is

$$\mathrm{Fe} \;+\; 2\mathrm{H_2O} \;\longrightarrow\; \mathrm{Fe(OH)_2} \;+\; \mathrm{H_2}\,.$$

In chemical equilibrium we have

$$\frac{p_{\mathrm{Fe(OH)_2}}\, p_{\mathrm{H_2}}}{p_{\mathrm{Fe}}\, p_{\mathrm{H_2O}}^2} = \mathrm{e}^{-\Delta G/RT} = K_p(\mathrm{Fe(OH)_2})\,. \tag{24}$$

The limit curve in the P-T-plane where one half of the Fe available in the gas phase is converted into $Fe(OH)_2$ is obtained by letting $p_{\mathrm{Fe}} = p_{\mathrm{Fe(OH)_2}}$ in (24). The partial pressure of H_2O in the gas phase is

$$\begin{aligned} p_{\mathrm{H_2O}} = \big[& \epsilon_{\mathrm{O}} - \epsilon_{\mathrm{C}} - (1 + f_{\mathrm{qu}} + 2f_{\mathrm{py}} + 3f_{\mathrm{ol}})\epsilon_{\mathrm{Si}} \\ & -[(1 - f_{\mathrm{ir}})\epsilon_{\mathrm{Fe}} + (2(1 - x_{\mathrm{ol}}) f_{\mathrm{ol}} + (1 - x_{\mathrm{py}}) f_{\mathrm{py}})\epsilon_{\mathrm{Si}}]\big]\, P_{\mathrm{H}}\,. \end{aligned} \tag{25}$$

It follows

$$\begin{aligned} P \;=\; & \frac{1 + 2\epsilon_{\mathrm{He}}}{4K_p(\mathrm{Fe(OH)_2})}\Big(\epsilon_{\mathrm{O}} - \epsilon_{\mathrm{C}} - (1 - f_{\mathrm{ir}})\epsilon_{\mathrm{Fe}} - \\ & [1 + f_{\mathrm{qu}} + (1 + x_{\mathrm{py}}) f_{\mathrm{py}} + (1 + 2x_{\mathrm{ol}}) f_{\mathrm{ol}}]\epsilon_{\mathrm{Si}}\Big)^{-2}\,. \end{aligned} \tag{26}$$

This limit curve is shown in Fig. 2. The iron hydroxide molecule occurs at such a low temperature that iron condenses before this molecule consumes significant fractions of the gas phase iron. It needs not to be considered further in the context of iron condensation.

3. Grain growth

3.1. Formation of condensation centres

Dust formation is initiated by the clustering of molecular species from the gas phase into clusters consisting of roughly 10 . . . 100 atoms on which irreversible growth of gas phase species becomes possible. This nucleation process is the most difficult step in the chain of events which ultimately results in the condensation of solid dust grains. Since aggregates of this size are

usually less tightly bound than the bulk condensate, considerable supercooling below the stability limit of the corresponding solid material is required before the first seed nuclei are formed which then serve as centres for subsequent growth to macroscopic grains. If the gas phase consists of a mixture of several species from which at least some may condense into different solids, that material in a cooling environment which first starts to nucleate with a significant rate provides the required seed nuclei on which all other possible condensates may precipitate. The material which initiates dust formation needs not to be identical with the main dust material formed during subsequent growth on the initial seed nuclei, since even a rare component in the mixture can provide the required seed nuclei if these are formed at a higher temperature than for all other materials from which seed nuclei might be formed.

With respect to circumstellar shells around stars of spectral type M the chemical composition of the condensate is quite clear. For normal element abundances the dust mainly consists of compounds formed from O, Si, Fe, and Mg. Some dust may also be formed from less abundant elements, especially compounds of Al and Ca. Less clear is the process which initiates dust formation. The recent discussion of the problem of nucleation for M stars (Gail & Sedlmayr 1998a, 1998b) has shown that a direct nucleation involving the abundant gas phase species SiO, Fe, and Mg is not responsible for the observed circumstellar dust formation process, since formation of seed nuclei from these species occurs at much lower temperatures as that for which dust formation is observed to start in circumstellar dust shells. Nucleation in M stars, thus, involves molecular species from some less abundant elements. We have then shown (Gail & Sedlmayr 1998a) that the most likely processes for nucleation are formation of Al_mO_n and Ti_mO_n clusters and the results of a preliminary calculation presented in Gail & Sedlmayr (1998b) shows that cluster formation from TiO_2 molecules indeed occurs at temperatures above the stability limit of the condensates based on the metals Si, Fe, and Mg. Whether nucleation based on aluminium bearing molecules occurs at an even higher temperature than nucleation of titanium oxides is an open question since the required data for cluster bond energies for aluminium oxides presently are not available.

Independent from this uncertainty, it seems now clear that condensation of the abundant silicate dust seen in the IR emission from circumstellar shells condenses on seed nuclei which are formed already before the cooling track of the stellar wind crosses the stability limit of forsterite, which would be the first stable compound formed from the abundant elements O, Si, Mg, and Fe in chemical equilibrium in a cooling gas. Since the possible seed nuclei are formed at a temperature where aluminium already condenses, for instance, into corundum (Gail & Sedlmayr 1998b) there occurs already some growth of solid material on the initial seed nuclei before the onset of silicate growth. The growth of the visible dust then starts on particulates which most likely have already sizes of the order of nanometers.

There exists the possibility that the process of nucleation of seed particles has not yet come to a rest when silicate dust starts to condense. Without a detailed model for the kinetics of the nucleation process we cannot decide whether nucleation continues into the region of silicate formation. For simplicity we assume in our model calculation that all seed nuclei are formed prior to the onset of silicate condensation.

3.2. Dust species

In this paper we consider the formation of the visible dust in shells around M stars. From considerations of equilibrium condensation as in Sect. 2 we expect that the main dust component is a magnesium-iron silicate with composition $Mg_{2x}Fe_{2(1-x)}SiO_4$. In chemical equilibrium the iron content of this olivine would be negligible small, at least under conditions encountered in the condensation zone. In a circumstellar dust shell the dynamical timescale is not long compared to possible growth time scales. Then, since the initial abundance of Mg and Fe in the gas phase are nearly equal to each other, we must take into consideration that initially much more iron is built into the lattice during the grain growth process than in a chemical equilibrium state and that subsequent evolution to the equilibrium composition may be too slow compared to the dynamical timescale. Additionally we observe that since the abundance of Si also is nearly equal to the iron and magnesium abundance, there is not enough Mg available to condense all the Si into pure forsterite (Mg_2SiO_4). The iron content of the olivine also for this reason needs to be higher than in thermodynamic equilibrium. Thus, we consider the formation of olivine with a composition x different from its composition in an equilibrium state, which then has to be determined from the kinetics of the growth processes.

We do not consider the possible formation of pyroxene ($Mg_xFe_{1-x}SiO_3$) since this material hat not been found to be formed in condensation and subsequent annealing of laboratory analogues of circumstellar condensates (Day & Donn 1978, Nuth & Donn 1982a, Hallenbeck et al. 1998, see however Rietmeijer et al. 1986). In chemical equilibrium this compound would take up a big part of the Si and Mg and since the (Mg+Fe)/ Si ratio in pyroxenes is unity and the iron content in equilibrium is small, most of the iron would condense as the free metal if substantial amounts of pyroxene are formed.

If no pyroxenes are formed, much of the iron is consumed in the formation of olivine. Indeed, for Solar System abundances as given by Anders & Grevesse (1989) the combined Mg and Fe abundance is insufficient to condense all Si into olivine. In a stellar wind the degree of condensation of the silicon into solids never reaches a value near unity for the following reason: Once a certain fraction of the silicon is condensed into dust the radiation pressure on the dusty gas exceeds the gravitational pull of the star (usually 20% condensation of Si into dust is required for this). The gas then is rapidly accelerated to highly supersonic outflow velocities with the consequence that the gas is rapidly diluted and growth timescales become prohibitive long for further condensation. Part of the Si then remains in the gas phase and is incorporated into grains only much later if the stellar wind material has long become part of the interstellar matter. The iron and magnesium from the gas phase then is not com-

pletely consumed by silicate dust formation. Since solid iron itself becomes stable at temperatures only slightly below the stability limit of the silicates, it is to be expected that in a stellar wind part of the iron condenses into solid iron dust grains. For this reason we consider in our calculation the formation of a separate iron dust component.

Solid iron forms with Ni a solid solution with a small negative enthalpy of solution (cf. Saxena & Ericksson 1986). This means that Ni atoms from the gas phase are easily incorporated into iron grains. Since the Ni abundance for a standard element mixture is 5% that of iron and since part of the iron is bound in the silicate dust component, the iron grains should contain a significant fraction of Ni. We do not consider this additional complication in this paper and treat the iron grains as being pure iron.

As we have seen, an additional condensate which may be formed from the SiO molecules in the stellar wind is quartz (SiO_2) which would condense at rather high temperatures from the gas phase. Though quartz is not found to be formed in calculations of the chemical equilibrium composition of solid-gas mixtures with standard element abundance (e.g. Saxena & Ericksson 1986, Sharp & Huebner 1990) since formation of the Mg-Fe-silicates is thermodynamically more favourable, it nevertheless may condense in the stellar wind since condensation occurs under non-equilibrium conditions where only part of the gas-phase SiO is consumed by formation of the Mg-Fe-silicates. In this case some fraction of the SiO may condense into quartz. For this reason we consider in our calculation the formation of a separate quartz dust component. For the same reason we also consider the formation of periclase.

Other dust components than olivine, iron, and quartz are not considered, though some might be formed in small amounts, especially Al-Ca compounds. Also, we do not consider the possible conversion of the iron grains into iron sulfide or oxide grains at temperatures well below the condensation temperature. Some estimates which show the latter processes to be unlikely to occur in circumstellar shells are presented in Gail & Sedlmayr (1998a).

3.3. Growth of silicate dust grains

We assume that silicate dust grows by vapour deposition on the surface of some pre-formed seed nuclei. The seed nuclei are assumed to be spheres with a monodispersed size distribution with radius a_0. These seed nuclei likely are nano-sized corundum grains, which in turn may have grown on titanium oxide clusters. The precise chemical nature of these seed nuclei is not important in what follows.

Since the nominal monomer of olivine does not exist, the silicate grows by addition of SiO, Mg, Fe, to the surface and by oxidation with water vapour from the gas phase. The net reaction is

$$2x\mathrm{Mg} \;+\; 2(1-x)\mathrm{Fe} \;+\; \mathrm{SiO} \;+\; 3\mathrm{H_2O} \longrightarrow \mathrm{Mg_{2x}Fe_{2(1-x)}SiO_4(s)} \;+\; 3\mathrm{H_2}\,. \tag{27}$$

The details of the surface reactions involved in the silicate growth are not known. We assume here that the rate determining step of the total growth process is the deposition of a SiO molecule on the surface. The deposition rates per unit time and surface area for a particle in rest with respect to the gas phase are

$$J^{\rm gr}_{\rm SiO} = \alpha_{\rm SiO} n_{\rm SiO} v_{\rm th,SiO} \tag{28}$$

$$J^{\rm gr}_{\rm Mg} = \alpha_{\rm Mg} n_{\rm Mg} v_{\rm th,Mg} \tag{29}$$

$$J^{\rm gr}_{\rm Fe} = \alpha_{\rm Fe} n_{\rm Fe} v_{\rm th,Fe} \tag{30}$$

$$J^{\rm gr}_{\rm H_2O} = \alpha_{\rm H_2O} n_{\rm H_2O} v_{\rm th,H_2O}\,. \tag{31}$$

α denotes the sticking coefficient, n the particle density in the gas phase and v is the root mean square thermal velocity of the particles

$$v = \sqrt{\frac{kT}{2\pi m}}\,. \tag{32}$$

If the rate determining step for silicate growth is SiO addition all other deposition rates adjust to this rate and the growth rate for spherical grains of radius a is

$$\frac{1}{V_0}\frac{\mathrm{d}}{\mathrm{d}t}\frac{4\pi a^3}{3} = 4\pi a^2\, J^{\rm gr}_{\rm SiO}\,. \tag{33}$$

V_0 denotes the volume of the nominal monomer in the solid, which is given by

$$V_0 = \frac{A m_{\rm H}}{\rho_D}\,. \tag{34}$$

A is the atomic weight of the monomer and ρ_d the mass density of the bulk condensate.

We determine the rate of the decomposition reaction of the silicates, which is the reverse of reaction (27), by a Milne relation from the growth rate. In an equilibrium state for each species the rate of loss by decomposition $J^{\rm dec}$ equals the rate of gain by growth from the gas phase $J^{\rm gr}$. If the rate determining step for silicate formation is SiO addition then the decomposition rate in a thermodynamic equilibrium state is given by

$$J^{\rm dec} = \alpha_{\rm SiO}\, v_{\rm SiO}\, \frac{p_{v,\rm SiO}}{kT} \tag{35}$$

where $p_{v,\rm SiO}$ is the partial pressure of SiO molecules in chemical equilibrium between the gas phase and the solid which is given by (7). The relation can also be applied if the dust grain is not in thermodynamic equilibrium with the gas if this rate is calculated for the internal lattice temperature T_d of the grain which may be different from the actual gas temperature T_g.

The equation for the radius change of spherical dust grains then is

$$\frac{\mathrm{d}a}{\mathrm{d}t} = V_0 \alpha_{\rm SiO} v_{\rm SiO}\left[n_{\rm SiO} - \frac{p_{v,\rm SiO}}{kT_g}\sqrt{\frac{T_g}{T_d}}\right]\,. \tag{36}$$

This equation has to be solved with the initial condition $a = a_0$ at the instant when for an outwards moving gas parcel the bracket on the r.h.s becomes positive.

If the dust grain moves with velocity V with respect to the gas, the growth rate has to be modified. The deposition rate $J^{\rm gr}_{\rm SiO}$ for SiO has to be replaced by $J^{\rm gr}_{\rm SiO} \cdot F(S)$ where $F(S)$ is a complicated function of the ratio $S = V/v_{\rm SiO}$ given, for instance, in Schaaf (1963). For practical purposes this can be replaced with an error of at most a few percent by the much simpler expression

$$F(S) = \sqrt{1 + \frac{\pi m_{\rm SiO}}{8kT_g} V^2}\,. \tag{37}$$

Eq. (36) then changes into

$$\frac{{\rm d}a}{{\rm d}t} = V_0 \alpha_{\rm SiO} v_{\rm SiO} \left[n_{\rm SiO} \sqrt{1 + \frac{\pi m_{\rm SiO}}{8kT_g} V^2} - \frac{p_{v,{\rm SiO}}}{kT_g} \sqrt{\frac{T_g}{T_d}} \right]\,. \tag{38}$$

3.4. Change of composition of olivine

Next we consider the composition of olivine particles with respect to the fractional abundance of Mg and Fe. The abundance ratio of the cations changes with time by particle growth and evaporation. Since olivine can be conceived as an ideal solution of forsterite (Mg_2SiO_4) and fayalite (Fe_2SiO_4) each site for a cation can either be occupied by an Fe^{++} or Mg^{++} ion. We then can assume that the probability x that a freshly created surface site for Mg or Fe during particle growth actually is occupied by Mg is given by the ratio of the deposition rates from the gas phase

$$x_g = \frac{\alpha_{\rm Mg} n_{\rm Mg} v_{\rm Mg}}{\alpha_{\rm Fe} n_{\rm Fe} v_{\rm Fe} + \alpha_{\rm Mg} n_{\rm Mg} v_{\rm Mg}}\,. \tag{39}$$

This does not necessarily equal the actual abundance x of Mg within the grain and, thus, particle growth changes the composition x at the grain surface. Vapourisation, however, does not change the surface composition of a grain since by this process Mg and Fe are ejected in proportions corresponding to their local abundance x in the grain surface.

In order to calculate the composition x of the olivine grains we follow the method outlined in Gail (1999). Let N denote the number of Si atoms within a silicate grain. The change of N with time by growth and decomposition is

$$\frac{{\rm d}N}{{\rm d}t} = 4\pi a^2 \left(J^{\rm gr} - J^{\rm dec} \right)\,. \tag{40}$$

Let M denote the number of sites for cations occupied by Mg^{++}. This number changes during growth and decomposition as

$$\frac{{\rm d}M}{{\rm d}t} = 4\pi a^2 \cdot 2 \cdot \left[x_g J^{\rm gr} - x J^{\rm dec} \right]\,. \tag{41}$$

The change of the probability x of occupation of the cation sites with Mg-ions is

$$\frac{{\rm d}x}{{\rm d}t} = \frac{\rm d}{{\rm d}t}\frac{M}{2N} = -\frac{M}{2N^2}\frac{{\rm d}N}{{\rm d}t} + \frac{1}{2N}\frac{{\rm d}M}{{\rm d}t} = -\frac{x}{N}\frac{{\rm d}N}{{\rm d}t} + \frac{1}{2N}\frac{{\rm d}M}{{\rm d}t}\,. \tag{42}$$

It follows

$$\frac{{\rm d}x}{{\rm d}t} = \frac{4\pi a^2}{N} \left(x_g - x \right) J^{\rm gr}\,. \tag{43}$$

Hence, by the growth and decomposition process the composition of both the grains and the gas phase changes until $x = x_g$ is achieved. Introducing the volume $4\pi a^3/3 = N V_0$ in (43) we obtain

$$\frac{{\rm d}x}{{\rm d}t} = \frac{3V_0}{a} \left(x_g - x \right)\, J^{\rm gr}\,. \tag{44}$$

The second process that changes the fractional abundance of Fe and Mg in the silicates is cation exchange: If for instance a magnesium atom collides with the surface of a silicate grain at a site which is occupied by a Fe^{++} cation the particles may exchange and the outcome of the scattering process is an iron atom in the exit channel. This process is exothermic because the enthalpy change of the reaction

$$Fe_2SiO_4(s) \,+\, 2Mg(g) \,\longrightarrow\, Mg_2SiO_4(s) \,+\, 2Fe(g) \tag{45}$$

is $\Delta H = -156.72\,{\rm kJ\,mole^{-1}}$ (data taken from Lide 1995). The replacement of iron cations by magnesium cations, thus, is exothermic with 0.81 eV per particle which favours the replacement of Fe by Mg. Let us consider this exchange processes from the point of view of chemical thermodynamics. In Gail (1998a) it is shown that the partial pressures of magnesium and iron in the gas phase in equilibrium with olivine of composition $Mg_{2x}Fe_{2(1-x)}SiO_4$ at temperature T have to satisfy the relation

$$\frac{p_{\rm Mg}}{p_{\rm Fe}} = {\rm e}^{-\Delta G/RT} = K_p(T) \tag{46}$$

where

$$K_p(T,x) = \exp\Big[-\frac{\Delta G({\rm fa}) - \Delta G({\rm fo})}{2RT} - \frac{\Delta G_{\rm mix}}{2(1-x)RT} \Big] \tag{47}$$

and

$$\Delta G_{\rm mix} = 2RT \left[x \ln x + (1-x) \ln(1-x) \right]\,. \tag{48}$$

$\Delta G({\rm fa})$ and $\Delta G({\rm fo})$ are the free enthalpies of formation of fayalite and forsterite, respectively, from the free atoms and $G_{\rm mix}$ is the entropy of mixing for two moles of cations. Thus, olivine grains with a given composition x are in equilibrium with the gas phase if and only if the partial pressure of magnesium atoms in the gas phase equals

$$p_{\rm Mg,eq} = p_{\rm Fe} \cdot K_p(T,x)\,. \tag{49}$$

If the actual partial pressure $p_{\rm Mg}$ exceeds its equilibrium value $p_{\rm Mg,eq}$ the grain is unstable with respect to replacement of the excess iron by magnesium, or vice versa.

The exchange rate of Fe by Mg per unit surface area during collisions of Mg with the grain surface is

$$J^{\rm ex}_{+} = n_{\rm Mg}\, v_{\rm th,Mg}\, \alpha^{\rm ex}\,. \tag{50}$$

$\alpha^{\rm ex}$ describes the probability of exchange of Mg and Fe in the scattering process. The rate for the reverse reaction is

$$J^{\rm ex}_{-} = n_{\rm Fe}\, v_{\rm th,Fe}\, \beta^{\rm ex}\,. \tag{51}$$

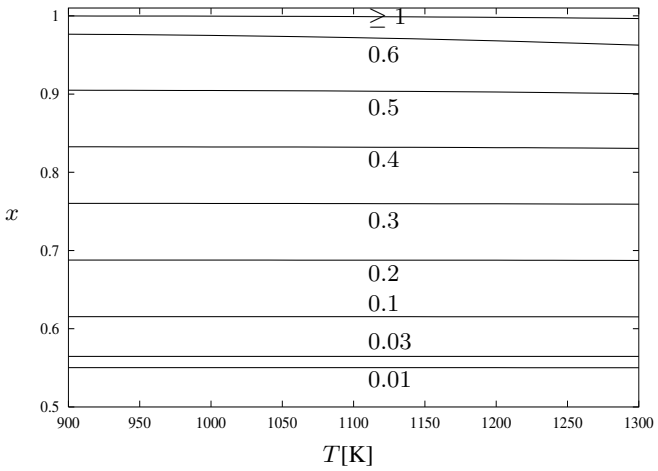

Fig. 3. Dependence of the initial composition x of olivine on temperature T and the ratio of the ion exchange coefficient $\alpha^{\rm ex}$ to the sticking coefficient $\alpha_{\rm SiO}$ for grain growth.

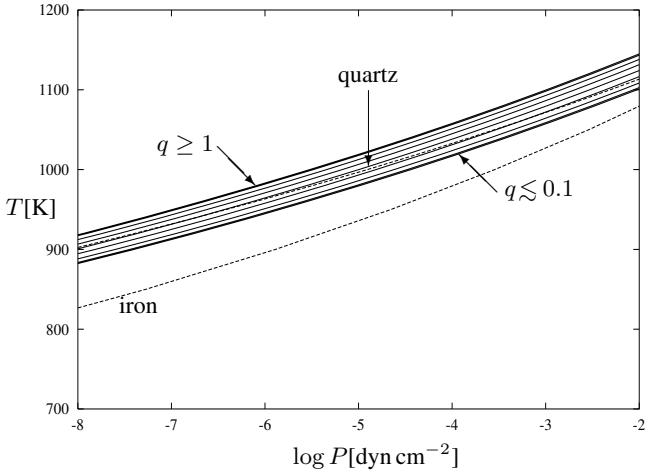

Fig. 4. Dependence of the condensation limit of olivine on the ratio q of the ion exchange coefficient $\alpha^{\rm ex}$ to the sticking coefficient $\alpha_{\rm SiO}$ for grain growth. The upper limit curve corresponds to nearly pure forsterite Mg_2SiO_4, the lower limit curve to olivine with a composition which approximately equals $MgFeSiO_4$. The intermediate curves correspond to the values of $\alpha^{\rm ex}/\alpha_{\rm SiO}$ in Fig. 3. The dashed curves show the stability limits of quartz and iron, for comparison.

In chemical equilibrium we have $J_+^{\rm ex} = J_-^{\rm ex}$ from which it follows

$$\beta^{\rm ex} = \alpha^{\rm ex} \frac{v_{\rm th,Mg}}{v_{\rm th,Fe}} \frac{n_{\rm Mg,eq}}{n_{\rm Fe}} \,. \tag{52}$$

$n_{\rm Mg,eq}$ is given by (49). The rate of change of the number M of surface sites occupied by Mg^{++} cations is

$$\frac{{\rm d}M}{{\rm d}t} = 4\pi a^2 \left(J_+^{\rm ex} - J_-^{\rm ex}\right) \,. \tag{53}$$

Adding this to the r.h.s of (41) yields our final equation for the change of the composition x of olivine

$$\frac{{\rm d}x}{{\rm d}t} = \frac{3V_0}{a} \left[(x_g - x)\; J^{\rm gr} + \tfrac{1}{2}\left(J_+^{\rm ex} - J_-^{\rm ex}\right)\right] \,. \tag{54}$$

The effective exchange rate is

$$J_+^{\rm ex} - J_-^{\rm ex} = v_{\rm th,Mg}\, \alpha^{\rm ex} \left(n_{\rm Mg} - n_{\rm Fe} K_p(T,x)\right) \,. \tag{55}$$

If diffusion within the grain is important, some modifications are necessary. This case is treated in Sect. 4.2.

3.5. Composition of olivine at the onset of grain growth

The vapour pressure of a solution depends on the concentration of the solvent, as is well known. For olivine this means that the stability limit where olivine starts to grow on the surface of seed nuclei depends on the composition of the olivine during the very first stage of grain growth. Comparing Eqs. (54) and (36) we see, that the characteristic timescale for grain growth and change of composition roughly are of the same order of magnitude. During the first stage of olivine growth the composition x then nearly equals the stationary equilibrium composition obtained from Eq. (54) by putting its left hand side to zero

$$x = x_g + \frac{J_+^{\rm ex} - J_-^{\rm ex}}{2J^{\rm gr}} \,. \tag{56}$$

The consumption of SiO, Fe, and Mg from the gas phase may be neglected during the initial phase of grain growth and we can take the partial pressures of these particles equal to the abundances of the elements Si, Fe, Mg[2]. Then we obtain the following equation for the initial composition x of olivine

$$x = x_g + \frac{1}{2}\,\frac{\alpha^{\rm ex}}{\alpha_{\rm SiO}}\,\frac{\epsilon_{\rm Mg} - \epsilon_{\rm Fe} K_p(T,x)}{\epsilon_{\rm Si}} \sqrt{\frac{m_{\rm SiO}}{m_{\rm Mg}}} \,. \tag{57}$$

This determines x for given temperature T and composition of the gas phase. It determines the initial value to be used in the integration of (54).

Fig. 3 shows the dependence of x on T and the ratio of the ion exchange coefficient $\alpha^{\rm ex}$ to the sticking coefficient $\alpha_{\rm SiO}$ for grain growth. The dependence on T is only weak; x is mainly determined by the ratio $\alpha^{\rm ex}/\alpha_{\rm SiO}$. If this ratio is ≥ 1 the composition of the forsterite–fayalite solution is determined by the ion exchange processes at the surface. In this case the composition is as in chemical equilibrium and x is close to unity since in equilibrium olivine is nearly pure forsterite. If $\alpha^{\rm ex}/\alpha_{\rm SiO} \ll 1$ the composition is determined by growth processes and x equals its value x_g for the gas phase.

This initial value for x determines the limit for the onset of olivine condensation. For given temperature T Eq. (57) determines x and from (9) with $f_{\rm ol} = 0$ we obtain the total pressure P at the stability limit of olivine. Fig. 4 shows the dependence of the stability limit on the ratio $\alpha^{\rm ex}/\alpha_{\rm SiO}$. At a fixed gas pressure there is a temperature difference of 50 K between the condensation temperatures of olivine with a composition corresponding to the two limit cases Mg_2SiO_4 and $MgFeSiO_4$, which are formed if ion exchange either is efficient ($\alpha^{\rm ex}/\alpha_{\rm SiO} \geq 1$) or

[2] Some fraction of the Mg and Si may be bound into Ca-Al-compounds at the onset of olivine growth, but taking this into account would introduce only minor corrections and is neglected in this calculation

completely inefficient ($\alpha^{\rm ex}/\alpha_{\rm SiO} \ll 1$). This is not a small difference which may result in observable differences for models of circumstellar dust shells. Which case is realised is presently unknown. Since there is no obvious reason why exchange of Fe^{++} and Mg^{++} should be much less efficient then grain growth, we expect that $\alpha^{\rm ex} \approx \alpha_{\rm SiO}$. Our choice of $\alpha^{\rm ex}$ is given in Sect. 5.5.3.

3.6. Growth of iron grains

Next we consider the formation of iron grains. A direct nucleation of iron clusters from the gas phase and subsequent growth of iron particles as formation mechanism for iron grains can be excluded. Iron nucleation would occur at temperatures of the oder of 500 K (John & Sedlmayr 1997, Gail & Sedlmayr 1998a) where already large amounts of silicate dust are formed. In this case iron will condense by precipitation on the surface of the grains which are already present when the iron vapour becomes unstable with respect to condensation. It seems unlikely that silicates condense only on some part of the pre-formed seed nuclei such that some of them are left which may then act as growth centres for iron grains. Hence it is to be expected that iron precipitates on the surface of silicate grains and grows in competition with the substrate. Since the stability limit for iron condensation occurs at a temperature only 50 ... 100 K below the stability limit of the silicates (cf. Fig. 4) the growth of silicates is not yet finished if iron starts to condense. This means that iron condensation, if it occurs, has to operate simultaneously with silicate growth at the surface of silicate grains.

This can only occur if at the surface of the silicate grains part of the iron particles adsorbed to the surface and moving around are not incorporated into the silicate but associate with small iron island adhered to the silicate surface. The formation of such iron islands at the surface is not unlikely since thermodynamically it is more favourable for the olivine to build Mg into the lattice instead of Fe. The iron atoms which are adsorbed from the gas phase, but are not used for iron growth, or which first are incorporated into the silicate surface but then are replaced by magnesium, may hit such an iron island and stick to its surface before being desorbed from the silicate surface. There arise two questions in this context:

- how does such an island forms by surface nucleation and
- how long does it exist on the surface until it either is overgrown by a silicate layer or it splits off from the surface due to the build up of strong mechanical stresses at the boundary between iron and the silicate which may occur during irregular growth, or it is stripped off from the surface during grain-grain collisions.

It seems to us plausible that part of the iron particulates forming on the surface of the silicate grains later form tiny metallic inclusions within the silicate grains while some others attain to the gas phase, growing there as an independent dust species, but we cannot prove this presently. These questions can only be answered by a detailed study of the kinetics of the surface growth of olivine and iron and the microscopic structure of the surface which is out of the scope of the present paper. We study the possibility of simultaneous iron condensation besides silicate formation by simply assuming a prescribed number of growth centres and calculating the condensation of iron on these centres. We leave the question open whether the resulting iron particles are formed as separate grains or as inclusions within the silicate grains.

The growth of iron grains then is calculated by solving the analogue of equation (38) where all quantities now refer to Fe atoms instead of SiO.

Iron has often been speculated to form a separate dust component in circumstellar shells (eg. Jones 1990 and references therein). The recent detection of iron and troilite inclusions in glassy silicate grains of presumably interstellar origin (Bradley 1994, cf. also the discussion in Martin 1995, Goodman & Whittet 1995) supports the assumption that metallic iron grains do form in circumstellar dust shells. Also the models for the composition of interstellar dust discussed by Mathis (1996) indicate that iron grains form a component of the interstellar dust mixture.

3.7. Growth of quartz grains

With respect to formation of quartz grains we are confronted with the same basic problem as in the case of iron grains: Direct nucleation from the gas phase and subsequent growth as a separate dust component would occur at temperatures below 500 K (Gail & Sedlmayr 1998a). Quartz then would, if ever, condense onto the already existing grains.

The stability limit for quartz may either be lower or higher than the stability limit of olivine. If the ratio of the ion exchange coefficient $\alpha^{\rm ex}$ to the sticking coefficient $\alpha_{\rm SiO}$ for olivine growth exceeds approximately 0.3 the stability limit of olivine occurs at a higher temperature than that of quartz (cf. Fig. 4). The magnesium abundance in olivine then is $x \gtrsim 0.8$ (cf. Fig. 3). In the opposite case olivine starts to condense at a lower temperature than quartz. The order of the first appearance of quartz and olivine, thus, depends on the unknown value of the exchange coefficient α^{ex}. We assume in this paper $\alpha^{\rm ex} \approx \alpha_{\rm SiO}$ in which case olivine condenses first. Growth of quartz and olivine, then, should occur simultaneously at the same surface. It does not seem impossible that a mixed material of microcrystallites, partially with the composition of olivine, partially with that of quartz, grows from the gas phase. The condensation experiments of Nuth & Donn (1982a) or Hallenbeck et al. (1998) seem to indicate that this may really be possible. In order for studying the possibility of growth of a quartz dust component we, again, simply assume a prescribed number of growth centres and calculate the condensation of quartz on these centres by solving the analogue of equation (38) adapted to the case of growth of quartz grains.

4. Solid diffusion and annealing

For dust materials like olivine which form a solid solution of two (or more) components the concentrations of the different solution components may vary within the grain. In case of circumstellar grains such concentration gradients arise from a change

of concentration of the growth species in the gas phase during grain growth or a shift of the equilibrium concentration of the solution components of the mixture with a changing temperature experienced by a grain during the outflow. Concentration gradients within the dust grains may have significant effects on the properties of the grains and the distribution of the solution components between the condensed phase and the gas phase and, thus, have to be considered in a calculation of circumstellar grain growth.

On the other hand, concentration gradients gives rise to the effect of concentration diffusion within the grain which tends to smooth out local concentration differences. The actual spatial variation of the concentration of the solution components then is determined by the interplay between exchange processes of the solution components between the condensed and the gas phase at the surface of a dust grain and the transport of solution components within the grain by solid diffusion. In the following we describe how the composition of an olivine grain in a circumstellar dust shell can be calculated.

4.1. Diffusion within dust grains

Olivine has the composition $Mg_{2x}Fe_{2(1-x)}SiO_4$. Since the anions SiO_4^{4-} forming the backbone of the silicate lattice are the same for both solution components, forsterite (Mg_2SiO_4) and fayalite (Fe_2SiO_4), the composition differences within the mineral refer to the local concentrations $2x$ of Mg^{++} and $2(1-x)$ of Fe^{++} cations. Hence, we have to consider the diffusion of these ions within the lattice. We do not consider at this place self diffusion of the SiO_4 anions which, however, may be important for annealing of an amorphous structure. A spatial variation of x gives rise to a current density of magnesium and iron ions which is given within the frame of the usual approximations by

$$j_{\rm diff} = -nD \cdot 2\,\frac{\partial x}{\partial \boldsymbol{r}}\,, \tag{58}$$

where n is the total particle density, in the present case that of magnesium and iron cations, and D is the diffusion coefficient. By means of the continuity equation we obtain for instance for the particle density of magnesium cations

$$\frac{\partial n_{\rm Mg^{++}}}{\partial t} = 2n \frac{\partial}{\partial \boldsymbol{r}}\, D\, \frac{\partial x}{\partial \boldsymbol{r}}\,. \tag{59}$$

If we assume n to be constant and observe $n_{\rm Mg^{++}}/n = 2x$ then we obtain

$$\frac{\partial x}{\partial t} = \frac{\partial}{\partial \boldsymbol{r}}\, D\, \frac{\partial x}{\partial \boldsymbol{r}}\,. \tag{60}$$

For spherical grains this diffusion equation reduces to

$$\frac{\partial x}{\partial t} = \frac{1}{r^2}\,\frac{\partial}{\partial r}\, r^2\, D\, \frac{\partial x}{\partial r}\,. \tag{61}$$

This describes the redistribution of Mg^{++} and Fe^{++} cations in the interior of a grain by diffusion processes. For its solution we require appropriate initial and boundary conditions for x.

The boundary condition at the grain surface is determined by the grain growth process and by exchange processes of the solution components with the gas phase. This is considered in the next section. A second boundary condition is required in the interior of the grain. It depends on whether the specific dust material under consideration formed directly by nucleation from the gas phase or grew on a seed nuclei of a different composition. In the first case the dust consists throughout of the same material and the diffusion current (58) in this case has to vanish for symmetry reasons at the centre. This requires

$$\left.\frac{\partial x}{\partial r}\right|_{r=0} = 0\,. \tag{62}$$

If at the centre there is a seed particle which does not mix with the material of the outer dust particle the diffusion current has to vanish at the surface of the seed particle. According to (58) this requires

$$\left.\frac{\partial x}{\partial r}\right|_{r=r_0} = 0\,. \tag{63}$$

This is essentially the same boundary condition as (62) though the physical reasons from which they originate are different.

4.2. Boundary condition at the surface

In order to determine the boundary condition for the concentration of Mg^{++} cations at the surface of the grain we consider a short time interval Δt and determine the change of total number ΔN of nominal molecules and the number ΔM of Mg^{++} cations within the grain during Δt. For ΔN we obviously have

$$\Delta N = \int_S dS\, \left(J^{\rm gr} - J^{\rm dec}\right)\, \Delta t\,. \tag{64}$$

The integration is over the surface S of the grain. For ΔM we have according to the discussion in Sect. 3.4 for the contribution of vapourisation/decomposition and of ion exchange

$$\begin{aligned}\Delta M \;=\; &\left[2\int_S dS\, \left(x_g J^{\rm gr} - x_s J^{\rm dec}\right)\right.\\ &\left. + \int_S dS\, \left(J_+^{\rm ex} - J_-^{\rm ex}\right)\right]\, \Delta t\end{aligned} \tag{65}$$

where x_s denotes the concentration of Mg^{++} cations at the surface of the olivine grain. Additionally, diffusion of Mg^{++} from the interior of the grain into its surface layer, or from the surface layer into its interior, contributes to the change ΔM of Mg^{++} cations in the surface. This contribution is

$$-\frac{2}{V_0}\int_S dS\, D\, \boldsymbol{n} \cdot \frac{\partial x}{\partial \boldsymbol{r}}\, \Delta t$$

where $\boldsymbol{n}$ denotes the (outwards directed) normal unit vector of the surface.

The concentration x_s of Mg^{++} in the surface layer now is

$$x_s = \lim_{\Delta t \to 0} \frac{\Delta M}{2\Delta N}\,. \tag{66}$$

For spherical dust grains we obtain

$$x_s = \frac{2\left(x_g J^{\rm gr} - x_s J^{\rm dec}\right) + \left(J_+^{\rm ex} - J_-^{\rm ex}\right) - \frac{2}{V_0}\, D\, \left.\frac{\partial x}{\partial r}\right|_a}{2\left(J^{\rm gr} - J^{\rm dec}\right)} \tag{67}$$

which obviously may be written as

$$x(a) = x_g + \frac{J_+^{\rm ex} - J_-^{\rm ex}}{2J^{\rm gr}} - \frac{D}{V_0 J^{\rm gr}} \left.\frac{\partial x}{\partial r}\right|_{r=a} . \quad (68)$$

Since $J_-^{\rm ex}$ itself depends on $x(a)$, this is a complicated equation between the surface concentration $x(a)$ and the derivation of the concentration at the surface. Eq. (68) is the boundary condition for x at the grain surface which has to be prescribed for the solution of the diffusion equation (61). Except for the diffusive contribution it is identical with (57).

In order to see how this compares with our previous consideration in Sect. 3.4 we consider the total number M of all Mg^{++} cations in the grain

$$M = \frac{2}{V_0} \int dV\, x \quad (69)$$

and differentiate this with respect to time. For spherical particles we obtain

$$\frac{\partial M}{\partial t} = 2\frac{4\pi a^2}{V_0}\, x(a) \frac{{\rm d}a}{{\rm d}t} + 2\frac{4\pi}{V_0} \int_0^a dr\, r^2 \frac{\partial x}{\partial t} . \quad (70)$$

Substituting the diffusion equation (61) into the second term on the r.h.s. we obtain

$$\frac{\partial M}{\partial t} = 2\frac{4\pi a^2}{V_0} \left[x(a)\frac{{\rm d}a}{{\rm d}t} + D \left.\frac{\partial x}{\partial r}\right|_a \right] . \quad (71)$$

Inserting (67) for $x(a)$ and the equation for grain growth the terms depending on the concentration gradient at the surface cancel and we recover our result from Sect. 3.4 for the change of M with time. The concentration x in Sect. 3.4, thus, has the meaning of a mean concentration for the whole grain. This is identical with the true concentration, if diffusion is so fast that no concentration gradients develop within the grain. In this case Eq. (54) can be used to determine the composition of an olivine grain. If diffusion is not fast, the composition has to be determined by solving (61) subject to the boundary conditions (68) and(63).

4.3. Diffusion coefficient

Diffusion coefficients of several double valued cations in forsterite and some types of olivine have been measured in laboratory experiments. Of special interest in our case is the diffusion of Mg^{++} and Fe^{++} cations in olivine. According to Morioka (1981) the diffusion coefficient can be approximated by

$$D = D_0\, {\rm e}^{-E_D/RT - \alpha_c x} . \quad (72)$$

E_D is the activation energy for the internal hopping process within the lattice which results in cation diffusion. x is the concentration of the Mg^{++} cations and α_c is a constant describing the concentration dependence of the diffusion. The experimental results indicate that the concentration dependence of diffusion results from the formation of defects in the forsterite lattice in replacing Mg^{++} cations by different cations with different ionic radii (Morioka 1981). This enables diffusion via vacancies with increasing concentration of the substituents.

The coefficient α is slightly temperature dependent. From Fig. 5 of Morioka (1981) we take a value of $\alpha_c = 4.4$ at $T = 1\,100\,{\rm K}$ for Fe^{++} diffusion in olivine which we adopt for our calculations. For Mg self-diffusion α_c equals zero. The values for D_0 and E_D/R are different for different temperature regions. For Fe^{++} diffusion we take from Table 3 of Morioka (1981) the diffusion coefficient given for the lowest temperature region (900...1 000 K)

$$D_{\rm Fe} = 1.08\,10^{-2}\, {\rm e}^{-30300/T} \quad (73)$$

and for Mg^{++} self diffusion

$$D_{\rm Mg} = 1.82\,10^{-8}\, {\rm e}^{-17200/T} , \quad (74)$$

since for circumstellar dust shells only the low-temperature approximations are relevant. These coefficients have to be multiplied by $\exp(-\alpha_c x)$.

4.4. Annealing

As dust forms by growth from the gas phase, initial misalignments of the fundamental building blocks of the olivine minerals due to rapid growth later may be removed by internal hopping and re-arrangement process. This "annealing" tends to form a more homogeneous, crystalline lattice structure.

The characteristic timescale for annealing is

$$\tau_{\rm h}^{-1} = \nu {\rm e}^{-E_a/kT} . \quad (75)$$

ν is the number of attempts per unit time for hopping to a neighbouring lattice site or to change the orientation of a SiO_4 tetrahedron within the lattice. E_a is the activation energy barrier for this process. The characteristic activation energy for silicate materials has been estimated by Lenzuni et al. (1995) and Duschl et al. (1996) to be $E_a/k = 41\,000\,{\rm K}$ based on the annealing experiment of Nuth & Donn (1982a) for condensates from magnesium-silicate smokes and assuming the characteristic frequency ν to equal the average vibrational frequency $\nu = 2\,10^{13}\,{\rm s}^{-1}$ of the SiO_4 tetrahedron. The new laboratory experiments on silicate annealing of Hallenbeck et al. (1998) yield the same activation energy.

We assume that annealing proceeds by internal diffusion of SiO_4 tetrahedrons within the lattice and approximate this diffusion process by a 3D random walk on a cubic lattice. The diffusion coefficient in this case is

$$D = \frac{1}{3}\lambda^2 \nu {\rm e}^{-E_a/kT} \quad (76)$$

(e.g. Dekker 1963). λ is the average step length which we estimate from the volume V_0 of the basic molecule forming the lattice by $\lambda = V_0^{\frac{1}{3}}$. The molecular weight of Mg_2SiO_4 is $A = 140.7$ and its mass density $\rho = 3.21\,{\rm g\,cm^{-3}}$ (Lide 1995). We obtain for the coefficient of solid state diffusion within the silicate

$$D = 1.2\,10^{-2}\, {\rm e}^{-41\,000\,{\rm K}/T}\ [{\rm cm^2/s}] . \quad (77)$$

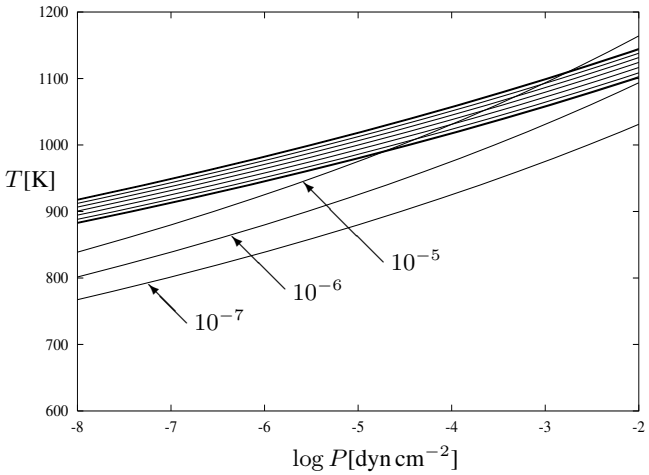

Fig. 5. Limit curves for formation of a locally ordered lattice structure during grain growth over distances Δa indicated at the curves. The upper set of curves are the stability limits of olivine for different efficiencies of ion exchange (compare Fig. 4).

The same estimate for D has been used in our previous papers Gail (1998a) and Gail & Sedlmayr (1998a).

For a crude estimate of the importance of the annealing process we compare the timescale required to deposit a new layer of thickness Δa on the grain

$$\tau_{\rm growth} = \Delta a \left| \frac{{\rm d}a}{{\rm d}t} \right|^{-1} \tag{78}$$

with the timescale required for annealing which we take to be the time

$$\tau_{\rm annealing} = \frac{(\Delta a)^2}{D} \tag{79}$$

required to move across the same distance Δa by a random walk. If $\tau_{\rm annealing}$ is shorter than $\tau_{\rm growth}$ we expect that a locally ordered lattice structure develops which extends at least over distances Δa. An ordered lattice structure then is expected if

$$\frac{\Delta a V_0 J_{\rm gr}}{D} < 1 \, .$$

For olivine growth this may be written as

$$P < kT \, \frac{D(1+2\epsilon_{\rm He})}{2\Delta a V_0 \alpha_{\rm SiO} v_{th,{\rm SiO}} \epsilon_{\rm Si}} \tag{80}$$

Above and to the left to the limit line in the p-T-plane defined by this relation the growth process is slower than internal re-arrangement processes within the lattice such that there is sufficient time for annealing of lattice defects which may result from irregular growth.

Some results for $\Delta a = 10^{-7}, 10^{-6}$, and 10^{-5} cm are shown in Fig. 5. For pressures of the order of 10^{-4} dyn cm^{-2}, typical for the condensation and initial growth zone in circumstellar dust shells, above $T \approx 900$ K the dust grains develop at least a microcrystalline ordered lattice structure over distances of the order $1 \ldots 10$ nm. If a substantial fraction of the total grain growth process occurs at lower temperatures, the grains develop over a crystalline core a thick amorphous outer mantle. If, on the other hand, most of the grain growth occurs above roughly 900 K the grains are expected to have an essentially microcrystalline structure. The outcome of the growth and annealing processes depends on the details of the cooling track and can only be predicted by model calculations. Obviously, both amorphous and micro-cristalline grains may be formed. Even monocrystalline grains may be obtained for suitable cooling tracks. This diversity of products of the growth process seems to be what is observed for circumstellar dust shells.

5. Model calculation

5.1. Model of the stellar wind

As a first application of the equations determining the condensation and composition of the dust in circumstellar shells we calculate the formation of a mixture of dust grains simultaneously with a simple model for the stellar wind. We consider the outflow from a single star with mass M_*, luminosity L_* and effective temperature $T_{\rm eff}$. The star is assumed to be not variable and the outflow to be stationary and spherically symmetric with a mass-loss rate $\dot{M}$. The mass density ρ and velocity v of the wind is determined by the equations of mass conservation

$$4\pi r^2 \, \rho v = \dot{M} \tag{81}$$

and momentum conservation

$$\rho v \frac{\partial v}{\partial r} = -\frac{\partial P}{\partial r} - \frac{GM_*}{r^2} \, [1-\Gamma] \, . \tag{82}$$

The ratio Γ of radiation pressure on the dusty gas to the gravitational pull of the central star is

$$\Gamma = \frac{L_*}{4\pi c G M_*} \, \kappa_{\rm H} \, , \tag{83}$$

where $\kappa_{\rm H}$ is the flux averaged mass extinction coefficient. Prior to condensation of significant amounts of dust one has $\Gamma < 1$ since the gas opacity is too small in order that radiation pressure exceeds gravitational attraction. If dust starts to condense Γ rapidly increases and if Γ becomes greater than unity radiation pressure on the dusty gas accelerates the gas-dust mixture to highly supersonic outflow velocities.

The pressure P is given by the ideal gas law

$$P = \frac{\rho k T}{\mu m_{\rm H}} \, . \tag{84}$$

$m_{\rm H}$ is the mass of the H atom and μ is the mean molecular weight. In order to avoid unnecessary complications of the solution resulting from the existence of a singular point through which the solution has to pass we neglect the pressure gradient in (82). Since in this approximation the velocity gradient is negative prior to the onset of significant dust condensation ($\Gamma < 1$) we assume

$$\frac{\partial v}{\partial r} = 0 \quad \text{if} \quad \Gamma < 1 \, . \tag{85}$$

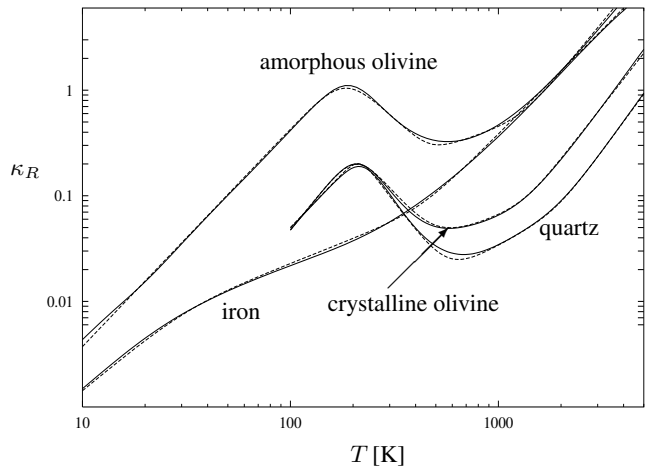

Fig. 6. Temperature variation of the Rosseland mean of the mass extinction coefficient for the indicated dust species (full lines) for an ensemble of grains with a MRN size distribution. The dashed lines show the analytic approximations for $\kappa(T)$ given in the text.

In this approximation the flow enters the condensation zone with some constant initial velocity v_0 and is accelerated to high outflow velocities once dust has formed.

The temperature structure in the dust shell is calculated in a strongly simplified way. First we do not discriminate between the lattice temperatures of the different dust species, which are usually different due to quite different absorption properties of the different dust species, but only use a single temperature T for all species. Second we assume the gas temperature also to equal this temperature T. Third we calculate T by the approximation given by Lucy (1971, 1976). The temperature in this case is given by

$$T^4 = \tfrac{1}{2} T_{\rm eff}^4 \left[1 - \sqrt{1 - \frac{R_*^2}{r^2}} + \tfrac{3}{2} \tau_L \right] \tag{86}$$

where τ_L is defined by

$$\frac{{\rm d}\tau_L}{{\rm d}r} = -\rho \kappa_{\rm H} \frac{R_*^2}{r^2} \tag{87}$$

and is subject to the boundary condition

$$\lim_{r \to \infty} \tau_L = 0 \,. \tag{88}$$

Eqs. (81) ... (88) completely specify the velocity and the P-T-stratification in the stellar wind, if the opacity $\kappa_{\rm H}$ is known. The problem depends on the parameters M_*, L_*, $T_{\rm eff}$, $\dot{M}$, and on the element abundances in the outflowing gas. In principle these parameters are uniquely determined by the initial mass of the star on the main sequence and its age. Presently the precise relations between the parameters are not yet known and it is more convenient to consider them to be free parameters for which we choose some typical values. Red Giants with optically thick dust shells start on the main sequence with masses between $\approx 2\,{\rm M}_\odot$ and $\approx 8\,{\rm M}_\odot$. Massive mass-loss and dust formation occurs on the top of the AGB when the stellar luminosity has climbed up to $L_* \gtrsim 10^4\,{\rm L}_\odot$. Since most of the stars observed in this phase have lost already a good part of their initial mass by the strong stellar wind we assume in this calculation $M_* = 1\,{\rm M}_\odot$ for the stellar mass. For the luminosity we assume a typical value of $L_* = 2\,10^4\,{\rm L}_\odot$. For $T_{\rm eff}$ we assume a value of 2 500 K which is representative for late type M stars (Dyck et al. 1974). The element abundances are chosen as Solar System abundances as given by Anders & Grevesse (1989) with the corrections of Grevesse & Noels (1993). Though dredge up processes carry up products of nuclear burning to the surface of the stars in the late phases of stellar evolution, the abundances of the elements O, Si, Mg, and Fe, from which the main dust components are formed, are not significantly affected by this as long as the star remains of spectral type M. The mass-loss rate $\dot{M}$ varies typically between 10^{-7} and a few times $10^{-5}\,{\rm M}_\odot\,{\rm yr}^{-1}$ (Loup et al. 1993). This parameter is varied in our model calculation.

5.2. Dust extinction

The extinction in Eqs. (83) and (87) is calculated by a simple superposition of the extinction of the different dust species and the gas

$$\kappa = f_{\rm ol}\kappa_{\rm ol} + f_{\rm si}\kappa_{\rm si} + f_{\rm ir}\kappa_{\rm ir} + f_{\rm qu}\kappa_{\rm qu} + \kappa_{\rm mol} \,. \tag{89}$$

$\kappa_{\rm ol}$, $\kappa_{\rm si}$, $\kappa_{\rm ir}$, and $\kappa_{\rm qu}$ are the mass extinction coefficients of crystalline olivine, amorphous olivine, iron, and quartz, respectively, if all of the Si or Fe is condensed into the indicated dust species. $f_{\rm ol}$, $f_{\rm si}$ and $f_{\rm qu}$ denote the fraction of the Si actually condensed into crystalline olivine, amorphous olivine, and quartz, respectively, and $f_{\rm ir}$ is the actual fraction of iron condensed into metallic iron grains. $\kappa_{\rm mol}$ is the extinction by the gas phase.

Absorption and scattering efficiencies $Q(a)$ for the different dust species are calculated for spheres of radius a by means of Mie theory. The complex dielectric coefficients required for this calculation for crystalline olivine and solid iron are taken from sources as described in Gail (1998a), the complex dielectric coefficient of amorphous olivine is taken from Dorschner et al. (1995) and that of quartz is taken from Brewster (1992). For a grid of wavelengths, at each grid-point the extinction coefficient is calculated for a grid of dust radii a and the resulting extinction coefficient for the different particle sizes is averaged by means of a Mathis-Rumpl-Nordsieck (Mathis et al. (1977) size distribution (MRN). From these results the Rosseland mean of the extinction coefficient is calculated. The results are shown in Fig. 6. The procedure of averaging $Q_\lambda(a)$ with a MRN distribution certainly is not very realistic for circumstellar dust shells, but since particle radii generally are small compared to the relevant wavelengths of the radiation field in a circumstellar dust shell, the extinction does not depend critically on the assumed particle size distribution. We can take the results to be representative for any distribution of *small* particles.

The extinction coefficient $\kappa_{\rm H}$ in Eqs. (83) and (87) is the flux average of the extinction coefficient. If optical depth in the dust shell are high this average approaches the Rosseland mean of the extinction coefficient. For this kind of average, however, the average of the extinction for a mixture of absorbers is not merely the superposition of the corresponding average of the

individual components as it is assumed in (89). Since, however, the extinction usually is dominated by one component of the mixture and dust extinction is rather smooth with respect to wavelength, the approximation (89) should be of sufficient accuracy for our present calculations, which are of a more explorative nature.

The mass extinction coefficients of the different dust materials for purposes of numerical calculations are approximated by analytical fit formulas. For crystalline olivine we have

$$\kappa_{\rm ol}(T) = \left[(6.147\,10^{-7}\,T^{2.444})^{-2} + \Big((6.957\,10^{4}\,T^{-2.329})^{2} + \sqrt{(3.505\,10^{-4}\,T^{0.755})^{4} + (1.043\,10^{-9}\,T^{2.523})^{4}}\Big)^{-1}\right]^{-\frac{1}{2}} \quad (90)$$

and for amorphous olivine we obtain

$$\kappa_{\rm si}(T) = \left[\frac{1}{\left(3.240\,10^{-5}T^{2.061}\right)^{2}} + \Big((2.092\,10^{4}T^{-1.836})^{4} + (4.265\,10^{-3}T^{.67})^{4} + (2.022\,10^{-8}T^{2.383})^{4}\Big)^{-\frac{1}{2}}\right]^{-\frac{1}{2}} \quad (91)$$

For iron we have

$$\kappa_{\rm ir}(T) = \left[\frac{1}{(3.341\,10^{-5}\,T^{1.632})^{4}} + \frac{1}{(6.405\,10^{-4}\,T^{.777})^{4} + (4.385\,10^{-7}\,T^{1.981})^{4}}\right]^{-\frac{1}{4}} \quad (92)$$

and for quartz

$$\kappa_{\rm qu}(T) = \left[\Big(\frac{1}{(3.898\,10^{-6}\,T^{2.054})^{4}} + \frac{1}{(3.100\,10^{5}\,T^{-2.622})^{4}}\Big)^{-\frac{1}{2}} + \Big((2.023\,10^{-5}\,T^{1.074})^{4} + (9.394\,10^{-11}\,T^{2.701})^{4}\Big)^{\frac{1}{2}}\right]^{\frac{1}{2}}. \quad (93)$$

These approximations fit the calculated values within a few percent accuracy in the whole temperature region $10\,{\rm K} \leq T \leq 3\,000\,{\rm K}$ as can be seen from Fig. 6.

The gas opacity is approximated by the fit formula for the Rosseland mean of the mass extinction by molecules

$$\kappa_{\rm mol} = 1\,10^{-8} \cdot \rho^{\frac{2}{3}} \cdot T^{3} \quad (94)$$

given by Bell & Lin (1994).

5.3. Chemical composition of the gas phase

We simply assume that H is completely associated to H_2, that carbon is completely bound in CO, that the silicon not condensed into solids is bound in SiO, that the oxygen not bound in Si, CO, and solids is bound in H_2O and that the Mg and Fe not bound in solids are present as free atoms. These are the dominating gas phase species in chemical equilibrium at temperatures around $T = 1\,000\,{\rm K}$ and pressures around $P = 10^{-4}\,{\rm dyn\,cm^{-2}}$ typically encountered in the condensation zone of circumstellar dust shells. These species should also be the most abundant gas phase species if chemical equilibrium does not apply for reasons of bond energies and element abundances. They are the most important species for dust growth with respect to formation of dust species from the Si-Mg-Fe complex.

There exist a lot of less abundant molecular species, but calculating their abundances from chemical equilibrium is not realistic and a fully non equilibrium calculation of the gas phase chemistry is out of the scope of the present paper.

Table 1. Data used in the calculation of growth and vapourisation rates

Substance	A	ρ_D	α	$\alpha^{\rm ex}$
Iron	55.845	7.87	1.0	
Quartz	60.085	2.196	0.01	
Forsterit	140.694	3.21	0.1	
Fayalite	203.774	4.30	0.1	0.06
Periclase	40.304	3.6	0.2	

A and ρ_D from Lide (1995), for α see text

5.4. Equations for the dust growth

We now present the complete set of equations for the time evolution of the abundances and compositions for the olivine, quartz, periclase, and iron dust component. The equations for the change of grain radii are

$$\frac{{\rm d}a_{\rm ir}}{{\rm d}t} = V_{0,\rm ir}\,(J^{\rm gr}_{\rm ir} - J^{\rm vap}_{\rm ir}) \quad (95)$$

$$\frac{{\rm d}a_{\rm qu}}{{\rm d}t} = V_{0,\rm qu}\,\left(J^{\rm gr}_{\rm qu} - J^{\rm dec}_{\rm qu}\right) \quad (96)$$

$$\frac{{\rm d}a_{\rm ol}}{{\rm d}t} = V_{0,\rm ol}\,\left(J^{\rm gr}_{\rm ol} - J^{\rm dec}_{\rm ol}\right) \quad (97)$$

$$\frac{{\rm d}a_{\rm pe}}{{\rm d}t} = V_{0,\rm pe}\,\left(J^{\rm gr}_{\rm pe} - J^{\rm dec}_{\rm pe}\right)\,. \quad (98)$$

The growth rates are

$$J^{\rm gr}_{\rm ir} = \alpha_{\rm ir} v_{\rm th,Fe}\, n_{\rm Fe} \quad (99)$$

$$J^{\rm gr}_{\rm qu} = \alpha_{\rm qu} v_{\rm th,SiO}\, n_{\rm SiO} \quad (100)$$

$$J^{\rm gr}_{\rm ol} = \alpha_{\rm ol} v_{\rm th,SiO}\, n_{\rm SiO} \quad (101)$$

$$J^{\rm gr}_{\rm pe} = \alpha_{\rm pe} v_{\rm th,Mg}\, n_{\rm Mg} \quad (102)$$

where

$$v_{\rm th} = \sqrt{\frac{kT}{2\pi m}}\,. \quad (103)$$

$n_{\rm Fe}$, $n_{\rm SiO}$, and $n_{\rm Mg}$ are the gas phase particle densities of Fe, SiO, and Mg, respectively. The vapourisation or decomposition rates are given by

$$J^{\rm vap}_{\rm ir} = \alpha_{\rm ir} v_{\rm th,Fe}\,\frac{p_{v,\rm Fe}}{kT} \quad (104)$$

$$J^{\rm dec}_{\rm qu} = \alpha_{\rm qu} v_{\rm th,SiO}\,\frac{p^{\rm qu}_{v,\rm SiO}}{kT} \quad (105)$$

$$J^{\rm dec}_{\rm ol} = \alpha_{\rm ol} v_{\rm th,SiO}\,\frac{p^{\rm ol}_{v,\rm SiO}}{kT} \quad (106)$$

$$J_{\rm pe}^{\rm dec} \;=\; \alpha_{\rm pe} v_{\rm th,Mg}\, \frac{p_{v,\rm Mg}^{\rm pe}}{kT}\,. \tag{107}$$

$p_{v,\rm Fe}$ is the vapour pressure of Fe atoms over solid iron, $p_{v,\rm SiO}$ is the partial pressure of SiO in the decomposition products of quartz and olivine at the given temperature T and composition x, and $p_{v,\rm Mg}$ is the partial pressure of Mg in the decomposition products of periclase. These partial pressures (different for each of the three species) can be calculated as indicated in Sect. 2. The equations for the change of the gas phase abundances of Fe, Mg, and SiO are

$$\begin{aligned}\frac{{\rm d}n_{\rm Fe}}{{\rm d}t} \;=\;& -4\pi a_{\rm ir}^2\, n_{d,\rm ir}\, (J_{\rm ir}^{\rm gr} - J_{\rm ir}^{\rm vap}) \\ & -4\pi a_{\rm ol}^2\, n_{d,\rm ol}\, 2\left((1-x_g)\, J_{\rm ol}^{\rm gr} - (1-x_{\rm ol}) J_{\rm ol}^{\rm dec}\right. \\ & \left. -\tfrac{1}{2}\left(J_{\rm ol,+}^{\rm ex} - J_{\rm ol,-}^{\rm ex}\right)\right) \end{aligned} \tag{108}$$

$$\begin{aligned}\frac{{\rm d}n_{\rm Mg}}{{\rm d}t} \;=\;& -4\pi a_{\rm ol}^2\, n_{d,\rm ol}\, 2\left(x_g\, J_{\rm ol}^{\rm gr} - x_{\rm ol} J_{\rm ol}^{\rm dec}\right. \\ & \left. +\tfrac{1}{2}\left(J_{\rm ol,+}^{\rm ex} - J_{\rm ol,-}^{\rm ex}\right) + J_{\rm pe}^{\rm gr} - J_{\rm pe}^{\rm vap}\right) \end{aligned} \tag{109}$$

$$\begin{aligned}\frac{{\rm d}n_{\rm SiO}}{{\rm d}t} \;=\;& -4\pi a_{\rm qu}^2\, n_{d,\rm qu}\left(J_{\rm qu}^{\rm gr} - J_{\rm qu}^{\rm vap}\right) \\ & -4\pi a_{\rm ol}^2\, n_{d,\rm ol}\,\left(J_{\rm ol}^{\rm gr} - J_{\rm ol}^{\rm dec}\right) \\ & -4\pi a_{\rm py}^2\, n_{d,\rm py}\,\left(J_{\rm py}^{\rm gr} - J_{\rm py}^{\rm dec}\right)\,. \end{aligned} \tag{110}$$

n_d is the particle density of the dust species. The equation for the change of the total water abundance in the gas phase is not considered; it is only important for the gas phase chemistry of other molecules from the gas phase which is not considered in this paper. The equation for the change of the composition of olivine is

$$\begin{aligned}\frac{{\rm d}x_{\rm ol}}{{\rm d}t} \;=\;& \frac{3V_{0,\rm ol}}{a_{\rm ol}}\Big[(x_g - x_{\rm ol})\; J_{\rm ol}^{\rm gr} \\ & +\tfrac{1}{2} v_{\rm th,Mg}\, \alpha_{\rm ol}^{\rm ex}\, (n_{\rm Mg} - n_{\rm Fe} K_p(T, x_{\rm ol}))\Big]\,. \end{aligned} \tag{111}$$

x_g is defined by (39).

These equations form a system of eight differential equations which determine the radii and composition of the grain species and the gas phase abundances of the relevant species Mg, Fe, and SiO. They have to be solved with appropriate initial conditions which are prescribed at the radius where the first dust species starts to condense. At this radius all particle radii are put to the radius a_0 of the seed nuclei. This is chosen arbitrarily as a_0=1 nm. For x we take as initial value the composition of olivine as determined by (57) at the point where the cooling track of the wind crosses the stability limit of olivine. With respect to the gas phase species see below.

For the calculation of the gas phase abundances we take advantage of the fact that we immediately can write down three first integrals of our system of equations. Since iron, for instance, either is bound in metallic iron grains and in olivine grains or it is present as the free atom in the gas phase, we have

$$\epsilon_{\rm Fe} = \frac{n_{\rm Fe}}{N_{\rm H}} + \frac{4\pi a_{\rm ir}^3}{3V_{0,\rm ir}}\frac{n_{d,\rm ir}}{N_{\rm H}} + 2(1-x_{\rm ol})\,\frac{4\pi a_{\rm ol}^3}{3V_{0,\rm ol}}\frac{n_{d,\rm ol}}{N_{\rm H}}\,. \tag{112}$$

$N_{\rm H}$ is the density of hydrogen nuclei. We calculate from this the gas phase density $n_{\rm Fe}$ of the iron atoms. Correspondingly

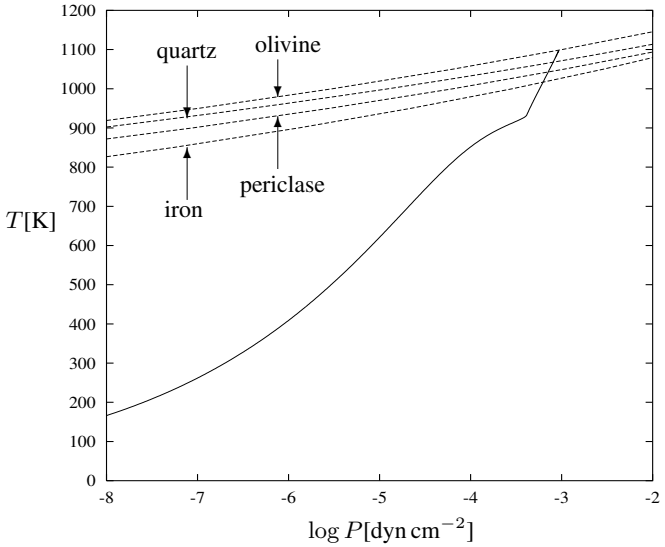

Fig. 7. Cooling track in the P-T-plane (full line) of the stellar wind with a mass-loss rate of $\dot{M} = 1\,10^{-5}\,{\rm M}_\odot\,{\rm a}^{-1}$. The dashed lines show the stability limits of crystalline olivine, quartz, periclase and iron.

we have for the total abundance of magnesium and silicon

$$\epsilon_{\rm Mg} \;=\; \frac{n_{\rm Mg}}{N_{\rm H}} + 2x_{\rm ol}\,\frac{4\pi a_{\rm ol}^3}{3V_{0,\rm ol}}\frac{n_{d,\rm ol}}{N_{\rm H}} + \frac{4\pi a_{\rm pe}^3}{3V_{0,\rm pe}}\frac{n_{d,\rm pe}}{N_{\rm H}} \tag{113}$$

$$\epsilon_{\rm Si} \;=\; \frac{n_{\rm SiO}}{N_{\rm H}} + \frac{4\pi a_{\rm ol}^3}{3V_{0,\rm ol}}\frac{n_{d,\rm ol}}{N_{\rm H}} + \frac{4\pi a_{\rm qu}^3}{3V_{0,\rm qu}}\frac{n_{d,\rm qu}}{N_{\rm H}}\,. \tag{114}$$

$n_{\rm Mg}$ and $n_{\rm SiO}$ are the gas phase particle densities of magnesium atoms and SiO, respectively. They are calculated from these two equations. Using these exact integrals instead of (108) ... (110) reduces the system of differential equations for the growth of dust to five differential equations coupled with some algebraic equations.

If the internal mixing ratio x of the two components forsterite and fayalite forming olivine is calculated one has to solve the diffusion equation (61) subject to the boundary conditions (63) and (68) instead of (111). The total system of equations to be solved then changes its character from a system of ordinary differential-algebraic equations into a system of partial differential-algebraic equations.

5.5. Numerical results

We have calculated a model for a stellar wind by solving simultaneously the set of Eqs. (95) ... (114) for the condensation and growth of dust and Eqs. (81) ... (88) for the outflow. We started the outwards integration at the stability limit where the first of the dust species condensing at the highest temperature (olivine or quartz, cf. Fig. 2) starts to condense. Except for very low $\alpha^{\rm ex}$ this usually turns out to be olivine. The calculation then follows the path of a gas parcel on its way out. As initial value for the velocity we choose in all calculations $v_0 = 1\,{\rm km\,s^{-1}}$, i.e., we assume that the gas enters the zone of condensation of the main dust components with roughly sonic velocity. The initial value of τ_L required for solving (87) was determined by a multiple

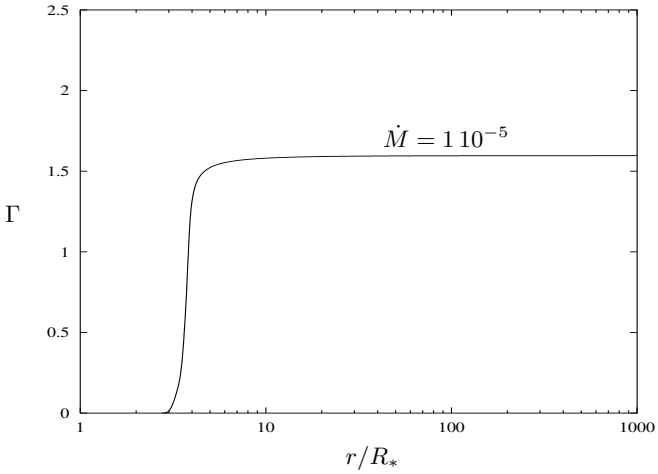

Fig. 8. Ratio Γ of radiation pressure to gravitational attraction in the wind.

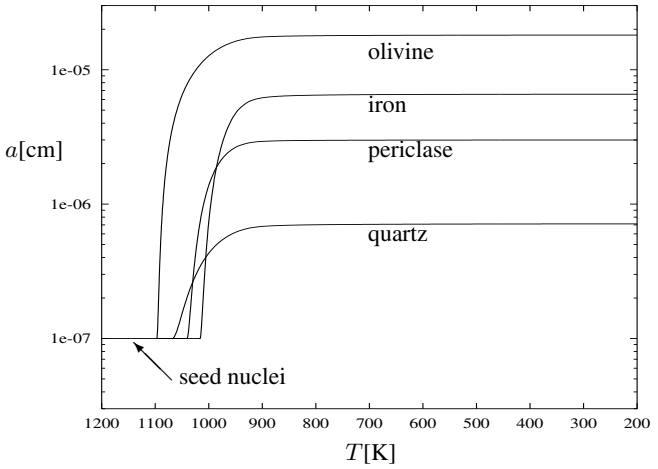

Fig. 9. Variation of the radii a for dust grains of the indicated species with dust temperature.

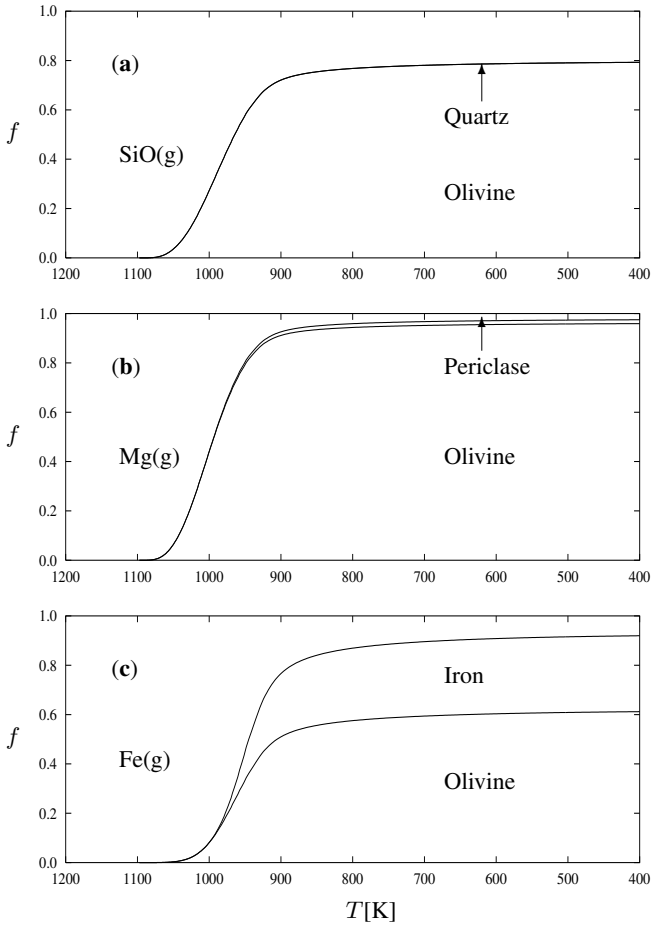

Fig. 10a–c. Distribution of the dust forming elements between the condensed minerals and the gas phase for an ion exchange coefficient of $\alpha^{\rm ex} = 0.6\alpha_{\rm gr}$: **a** Silicon, **b** Magnesium, **c** Iron.

shooting method until the boundary condition (88) is satisfied. The integrations were done by an Adams-Bashforth solver of third order accuracy (e.g. Golub & Ortega 1992) which requires only one evaluation of the r.h.s. of the equations for each time step. We did not use an error estimate for the choice of the time step size but rather determine step sizes from the condition that the most rapidly varying function changes by about 3% in each time step. The diffusion equation for iron cations in olivine is solved by standard methods Richtmyr & Morton 1967) using a fully implicit scheme. Some details are described in Appendix A. The solution of this partial differential equation coupled to the differential-algebraic equations for the wind and the dust growth offers no special problems.

5.5.1. Wind model

The model for the wind calculated on the basis of Eqs. (81) ... (88) is not very realistic since real dust forming stars with optically thick dust shells usually are variables. The following results of a model calculation for the wind should only be considered as a numerical experiment illustrating the formation of a multicomponent dust mixture in a simple model of a stellar outflow. Fig. 7 shows the cooling track of a stellar wind model for a mass-loss rate of $\dot{M} = 1\,10^{-5}\,{\rm M}_\odot\,{\rm yr}^{-1}$, which is representative for an object heavily obscured by an optically thick dust shell. This rate is near the upper limit of observed mass-loss rates for circumstellar dust shells around M stars (Loup et al. 1993). The dashed lines show the stability limits of the dust components considered in this calculation. If the cooling track of the wind crosses one of these limit curves, the corresponding dust component starts to condense. As can be seen from Fig. 7 the four dust components considered in this calculation start to condense in the following order: olivine, quartz, periclase, and iron.

Fig. 8 shows the ratio Γ of radiative to gravitational acceleration. This exceeds unity once substantial amounts of dust have been formed and the wind, then, is accelerated to highly supersonic velocities. The terminal outflow velocity in our model is $8.5\,{\rm km\,s}^{-1}$, which is within the frame of observed wind velocities.

5.5.2. Grain mixture

This calculation considers four dust species which may be formed from the most abundant elements (Si, Fe, and Mg) forming refractory compounds in an oxygen rich environment. These are olivine, quartz, iron, and periclase. The calculation assumes for all four components a density of seed nuclei of $n_d = 1\,10^{-13}$ per hydrogen nucleus. This number is rather arbitrary and chosen in such a way that the result for the final size of the olivine particles is roughly of the order of $0.1\,\mu$m. The precise number of the seed nuclei for olivine has to be calculated from a theory of nucleation which is not considered in this paper but will be discussed in a subsequent paper. The density of growth centres for quartz, iron, and periclase has to be derived from a theory of surface nucleation on olivine which is presently not at hand.

The sticking coefficient α for particle growth for olivine is chosen as 0.1 since Nagahara & Ozawa (1996) found that this gave the best fit for their experimental results. For iron we take the experimental value of $\alpha = 1$ at $T \approx 1\,000\,\mathrm{K}$ (Landolt-Börnstein 1968). For periclase we choose a value of $\alpha = 0.2$ which is near the upper range of experimental values given by Hashimoto (1990). For quartz we take $\alpha = 0.01$ from Hashimoto (1990) which is in accord with older experimental determinations (Landolt-Börnstein 1968).

Fig. 9 shows the radii of the four dust species for a stellar wind model with a mass loss rate of $\dot{M} = 1\,10^{-5}\,\mathrm{M}_\odot\,\mathrm{yr}^{-1}$, calculated with an ion exchange efficiency of $\alpha^{\mathrm{ex}} = 0.6\alpha_{\mathrm{gr}}$ (see below). The main dust component clearly is olivine, as is to be expected, but additionally a significant fraction of the iron condenses into metallic iron grains. A small fraction of the magnesium condenses into periclase grains. Quartz grains practically do not grow in the wind, which is a consequence of the small sticking efficiency α for this material.

The fraction of the elements Si, Mg, and Fe condensed into dust is shown Fig. 10. This shows that most of the silicon condenses into an iron rich olivine which consumes nearly all of the available magnesium but only part of the iron. The remaining fraction of the iron forms metallic iron grains. The amount of the magnesium condensed into periclase is only small. This material obviously does not form a major dust component.

These results depend to some extent on the ion exchange efficiency α_{ex}. Fig. 11 shows the distribution of the elements calculated with an exchange coefficient of $\alpha^{\mathrm{ex}} = 0.1\alpha_{\mathrm{gr}}$ instead of our preferred value of $\alpha^{\mathrm{ex}} = 0.6\alpha_{\mathrm{gr}}$. In this case, more iron condenses into metallic iron grains and a much bigger fraction of the magnesium condenses into periclase which, then, is one of the major condensates. Also in this case, formation of quartz grains can be neglected.

In their condensation experiment, Nagahara et al. (1988) found that the condensation products from the vapour of magnesium rich olivine in a hydrogen atmosphere were an iron rich olivine or pyroxene, metallic iron and silica (which at temperatures somewhat higher as that observed for circumstellar dust grains had the structure of tridymite). Qualitatively this fits well to the results of our calculation, except for quartz, which is most likely is found to be abundant in their experiment because of a much lower H excess in the gas phase.

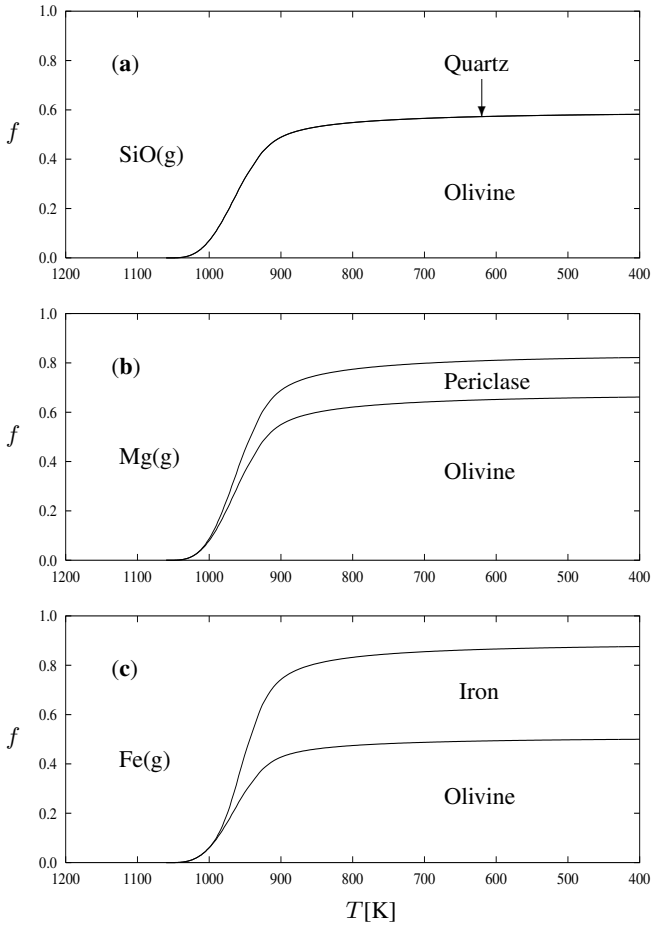

Fig. 11a–c. Distribution of the dust forming elements between the condensed minerals and the gas phase in case of a small ion exchange probability of $\alpha^{\mathrm{ex}} = 0.1\alpha_{\mathrm{gr}}$: **a** Silicon, **b** Magnesium, **c** Iron.

The particles obtained in the experiment of Nagahara et al. at temperatures $\gtrsim 1200\,\mathrm{K}$ are coarse grained, rectangular or platy, while at lower temperatures they found fine grained and rounded particles. This shows that our assumption that the grains grow as small spheres is not unrealistic.

5.5.3. Composition of the olivine

Fig. 12 shows some results of the calculations of the concentration x of magnesium cations in olivine grains. We solved the diffusion equation (61) with the temperature and concentration dependent diffusion coefficient according to Sect. 4.3. The concentration at the grain surface is calculated according to Eq. (68). Since the grain radius, at which the boundary condition (68) is prescribed, increases in time with a rate which depends to some extent (via the vapour pressure entering J^{vap}) on the composition x of the grain, we have to solve a strongly nonlinear diffusion problem with a free boundary. This is done by the method briefly outlined in Appendix A.

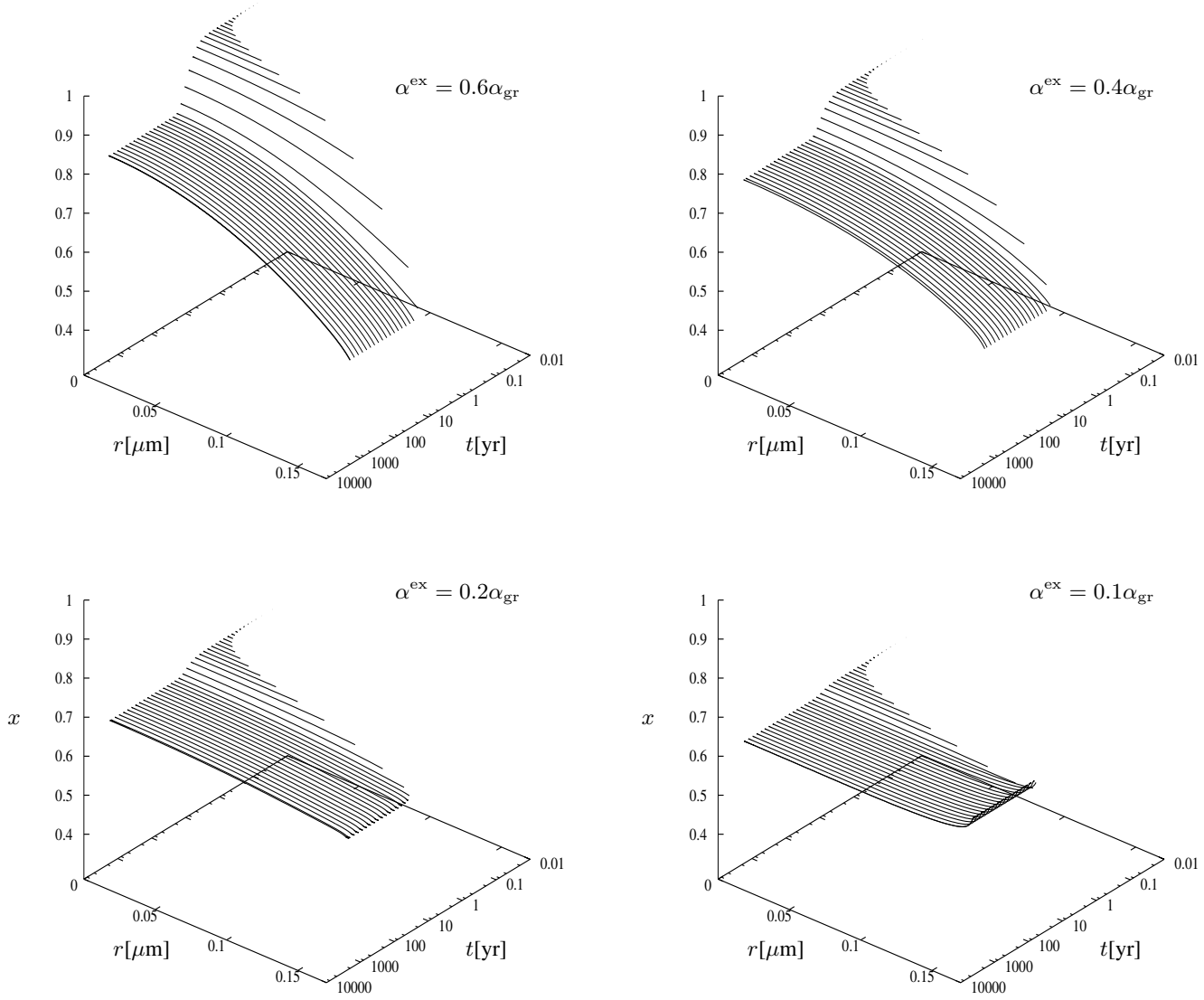

Fig. 12. Variation of the magnesium abundance x within an olivine grain ($Mg_{2x}Fe_{2(1-x)}SiO_4$) with the time elapsed (in years) since the onset of dust growth for four different values of the exchange coefficient $\alpha^{\rm ex}$. The values of $\alpha^{\rm ex}$ are shown in the figure.

Results are given for four different values of the exchange coefficient $\alpha^{\rm ex}$ of iron cations in favour of magnesium cations at the grain surface. For this quantity we have no direct information on its magnitude from experimental results. The experimental finding of Nagahara et al. (1988) that at high temperatures nearly pure forsterite condenses from an iron rich gas phase suggests that $\alpha^{\rm ex}$ cannot be small compared to the sticking coefficient for particle growth $\alpha_{\rm gr}$ (cf. Fig. 3). For our model calculations we choose for the exchange probability $\alpha^{\rm ex}$ a value of $0.6\,\alpha_{\rm gr}$ which guarantees a low but non-negligible iron content at higher temperatures, as it is observed in the experiments of Nagahara et al. A value of $\alpha^{\rm ex} \gtrsim \alpha_{\rm gr}$ would result in the formation of pure forsterite which is not observed in the experiments. The resulting internal compositional variation of olivine is shown in the upper left part of Fig. 12. For comparison we calculated the composition of the grains also for $\alpha^{\rm ex}/\alpha_{\rm gr} = 0.4$, 0.2, and 0.1. The results also are shown in Fig. 12. Significant variations of the Mg/(Fe+Mg) ratio within a grain occur only for $\alpha^{\rm ex} \gtrsim 0.2\alpha_{\rm gr}$. For lower values of $\alpha^{\rm ex}$ the particle composition is rather homogeneous and essentially reflects the element abundances of both elements.

Fig. 13 shows the magnesium abundance in olivine grains and in the gas phase for four different values of the exchange coefficient $\alpha_{\rm ex}$ as function of grain temperature. The full lines show the average magnesium abundance in the grain calculated from the solution of the diffusion equation (61) and the surface composition calculated from (68). The dashed line shows the gas phase composition.

The dotted line shows the average composition of the grain obtained by solving Eq. (111). The result of this calculation nearly exactly equals that calculated from a solution of the diffusion equation. A very small difference between the two results can be recognised in Fig. 13 for the case $\alpha^{\rm ex} = 0.6\alpha_{\rm gr}$ only, where a concentration gradient slightly modifies the surface

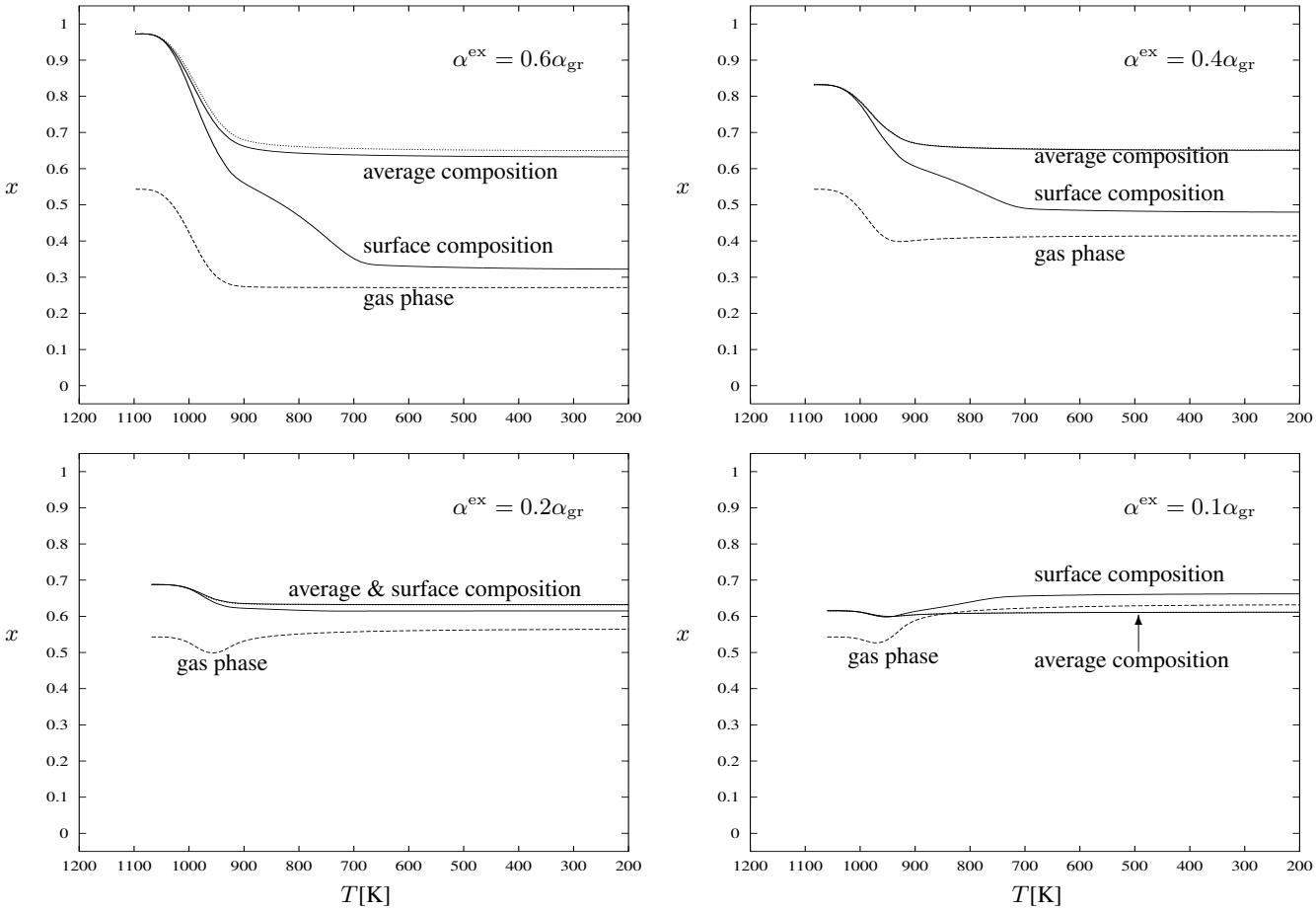

Fig. 13. Variation with dust temperature (radius) of the fraction x of cation sites in olivine occupied by magnesium at the grain surface and the average value of x for the whole grain calculated from the solution of the diffusion equation (full lines), the average value calculated by the equation (111) for the average x (dotted line), and the ratio $x_g = n_{\rm Mg}/(n_{\rm Mg} + n_{\rm Fe})$ for the gas phase (dashed line). Shown are results for the four indicated values of the exchange coefficient $\alpha^{\rm ex}$.

composition, an effect, which is not accounted for in Eq. (111). If only the average composition of the grain is required, it obviously suffices to solve (111) instead of the more complicated diffusion problem for the interior composition variations.

For $\alpha^{\rm ex} \gtrsim 0.4\alpha_{\rm gr}$, initially nearly pure forsterite is formed despite of a high iron abundance in the gas phase. With gradual depletion of the gas phase from magnesium due to its incorporation into grains the surface abundance of Mg starts to drop. First, this also leads to a reduced magnesium abundance in the grains interior by cation diffusion (cf. Fig. 12) but with decreasing temperature diffusion gradually becomes inefficient and there develops a considerable concentration difference of Mg^{++} between the grains surface and interior: A magnesium rich core then is surrounded by a thick iron rich rim.

For $\alpha^{\rm ex} < 0.4\alpha_{\rm gr}$ the particle composition does not vary much within the grain. Due to the negligible exchange of Fe^{2+} cations initially incorporated into the grain in favour of Mg^{2+} cations, the composition of the grains at each instant roughly equals the gas phase composition. For small $\alpha^{\rm ex}$ the magnesium abundance even slightly increases outwards since copious condensation of solid iron enhances the relative magnesium abundance in the gas phase. Fig. 11 shows for this case the distribution of the dust forming elements between the gas phase and the dust components. As compared to the case of an efficient ion exchange (cf. Fig. 10) obviously much more iron dust is formed and a significant fraction of the magnesium condenses into periclase.

Remarkably, the average iron and magnesium content of the olivine grains does not strongly depend on the magnitude of the ion exchange coefficient $\alpha^{\rm ex}$, but only the distribution of both elements within the grain.

Which case is realised, a high or a low ion exchange probability, can only be decided once information on the ion exchange probability from laboratory measurements is available. This, then, would allow to calculate the precise composition of circumstellar silicate grains and to predict abundance variations within grains which might become measurable once improved technics for detecting circumstellar material in meteorites and determination of their composition become available which allow also to detect silicate grains besides the already accessible aluminium compounds (cf. Nittler et al. 1997).

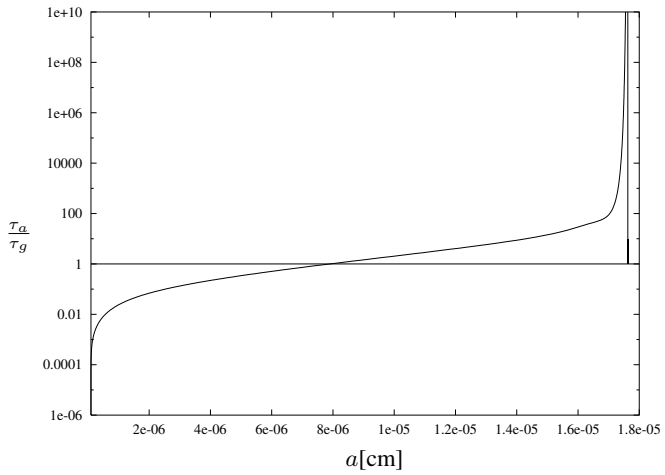

Fig. 14. Increase of the ratio of timescale for annealing τ_a to growth timescale τ_g with increasing grain radius a.

5.5.4. Annealing

Fig. 14 shows the variation of the ratio of the annealing timescale, defined by Eq. (79), to the growth timescale for olivine grains, defined by (78), as the grain radius increases during grain growth. For most part of the grain growth process this ratio is short enough, that the grains locally form an ordered lattice. Only during the final growth stage the temperature is too low to allow for internal rearrangement processes such that there develops an outer coating by amorphous material on a (micro)crystalline core.

We presently have taken this into account in calculating the extinction in a rather crude manner by using the extinction properties of crystalline olivine only. This introduces no serious error, despite of the big difference between the extinction properties of crystalline and amorphous olivine (cf. Fig. 6), since parallel to the formation of an amorphous rim, there form substantial amounts of metallic iron grains which absorb and scatter light at least as efficiently as amorphous olivine.

6. Concluding remarks

We have considered in this paper the condensation of a multicomponent mixture of mineral and metal grains in the stellar wind of a late type giant with an oxygen rich element mixture. The grains are assumed to grow on preformed seed nuclei the nature of which is left open in this paper. The nucleation problem is discussed in Gail & Sedlmayr (1998b) and will be discussed in more detail in a forthcoming paper of this series. We have not included in this paper the formation of aluminium dust grains which will be treated separately.

We have shown that not only silicate grains form in the wind, as usually is assumed, but that a substantial fraction of the iron condenses into separate grains of metallic iron. Also some periclase is formed. The formation of quartz turned out to be inefficient as a result of the measured low sticking efficiency.

The iron content of the olivine grains during the early stages of the growth process is low since cation exchange at the surface and internal cation diffusion ensures that the olivine composition always is close to the thermodynamic equilibrium composition. Only if the gas phase abundance of magnesium strongly decreases due to consumption in olivine grains with a resulting increase of the relative iron abundance in the gas phase, the exchange processes cannot keep pace with the growth process and the iron abundance of the grain material increases. The olivine grains develop a core mantle structure with an iron poor olivine material in the core and an iron rich material in the mantle. To what extent this leads to observable effects on the emitted IR spectrum will be discussed in a separate paper.

We have calculated the grain mixture and composition only for one wind model for a mass loss rate of $\dot{M} = 1\,10^{-5}\,\mathrm{M}_\odot\,\mathrm{yr}^{-1}$ since the present paper only discusses the basic system of equations. An extended set of model calculations including the radiative transfer in the dust shell will be discussed in a separate paper.

We presently have not considered the formation of pyroxene, though observationally the existence of a pyroxene dust component seems likely (Waters et al. 1996). The formation of this type of silicate material probably requires some solid state conversion process of olivine into pyroxene. For the rate of such a process we presently have no experimental data at hand.

Acknowledgements. Part of this work has been performed as part of a project within the *Sonderforschungsbereich 359 "Reaktive Strömungen, Diffusion und Transport"* which is supported by the Deutsche Forschungsgemeinschaft (DFG).

Appendix A: solution of the diffusion equation

Eq. (61) is discretised in fully implicit form as

$$x_j^n = x_j^{n-1} + \Delta t \left[A_j x_{j-1}^n + B_j x_j^n + C_j x_{j+1}^n \right] , \tag{A1}$$

where

$$A_j = \frac{r_{j-1}^2 D_{j-1} + r_j^2 D_j}{r_j^2 \left(r_j - r_{j-1}\right)\left(r_{j+1} - r_{j-1}\right)} \tag{A2}$$

$$B_j = -A_j - C_j \tag{A3}$$

$$C_j = \frac{r_j^2 D_j + r_{j+1}^2 D_{j+1}}{r_j^2 \left(r_{j+1} - r_j\right)\left(r_{j+1} - r_{j-1}\right)} . \tag{A4}$$

The superscript n refers to the time levels t_n, the subscript j ($1 \le j \le J$) to the radial grid points. $\Delta t = t_n - t_{n-1}$ is the step width in time. At the inner boundary of the grain at $j = 1$ we have according to (62) or (63)

$$x_1 = x_2 , \tag{A5}$$

at the outer boundary we prescribe

$$x_J = x_s \tag{A6}$$

where x_s is the solution of (68) where the derivative of x at the outer boundary is discretised as follows

$$\frac{\partial x}{\partial r} \to \frac{x_J^n - x_{J-1}^n}{r_J - r_{J-1}} . \tag{A7}$$

The resulting tridiagonal system of equations is solved by standard methods with taking care of avoiding rounding errors by the method proposed by Rybicki & Hummer (1991) (their Appendix A).

The x-dependence of the diffusion coefficient is taken into account by solving (A1) repeatedly with a diffusion coefficient calculated from the result of the last iteration step. This procedure usually converged within less than five iterations.

As radial grid points we use the radii $a(t_n)$ calculated from the solution of the growth equation for the dust particle radius. At time t_n this provides the n radii $a(t_n)$ which have been calculated at time steps $t_1 \ldots t_n$ which then are taken as our grid r_j at t_n. Thus, we have in each time step $J = n$ and $r_j = a(t_j)$. Our grid expands in this way at each time step by one point on which a value for x is provided by the boundary condition (68).

Our calculation of x is initialised as follows:

- For t_1 we have one grid point for which the value of x is defined by (68). The derivative of x in this equation has to be put to zero in this case since in a layer of zero width there is no concentration gradient.
- For t_2 we have two grid points $r_1 = a(t_1), r_2 = a(t_2)$. The value of x_2^2 follows from the outer boundary condition (68) and the value of x_1^2 from (A5).
- For t_3 we have three grid points $r_1 = a(t_1)$, $r_2 = a(t_2)$, $r_3 = a(t_3)$. The values of x_1^3 and x_3^3 are given by boundary conditions (68) at $j = J = 3$ and (A5) at $j = 1$, respectively. The value of x_2^3 is obtained from advancing x_2^2 to the new time level by means of (A1).

For all t_n with $n > 3$ we proceed analogously to the last step.

References

Anders E., Grevesse N., 1989, Geochimica et Cosmochimica Acta 53, 197

Begemann B., Dorschner J., Henning Th., et al., 1997, ApJ 476, 199

Bell K.R., Lin D.N.C., 1994, ApJ 427, 987

Bradley J.P., 1994, Sci 265, 925

Brewster M.Q., 1992, Thermal Radiative Transfer and Properties. John Wiley & Sons, New York

Day K.L., Donn B., 1978, ApJ 222, L45

Dekker A.J., 1963, Solid State Physics. Macmillan, London

Dominik C., Sedlmayr E., Gail H.-P., 1993, A&A 277, 578

Dorschner J., Begemann B., Henning Th., Jäger C., Mutschke H., 1995, A&A 300, 503

Duschl W.J., Gail H.-P., Tscharnuter W.M., 1996, A&A 312, 624

Dyck H.M., Lockwood G.W., Capps R.W., 1974, ApJ 189, 89

Gail H.-P., 1998, A&A 332, 1099

Gail H.-P., 1999, A&A, submitted

Gail H.-P., Sedlmayr E., 1998a, In: Hartquist T.W., Williams D.A. (eds.) The Molecular Astrophysics of Stars and Galaxies. Oxford University Press, p. 285

Gail H.-P., Sedlmayr E., 1998b, In: Sarre P. (ed.) Chemistry and Physics of Molecules and Grains in Space. Faraday Discussion 109, p. 303

Gilman R.C., 1969, ApJ 155, L185

Goebel J., Volk K., Gerbault F., et al., 1989, A&A 222, L5

Goebel J.H., Bregman J.D., Witteborn F.C., 1994, ApJ 430, 317

Golub G.H., Ortega J.M., 1992, Scientific Computing and Differential Equations. Academic Press, Boston

Goodman A.A., Whittet D.C.B., 1995, ApJ 455, L181

Grevesse N., Noels A., 1993, In: Prantzos N., Vangioni-Flam E., Cassé M. (eds.) Origin and Evolution of the Elements. Cambridge University Press, Cambridge, p. 15

Grossman L., 1972, Geochimica et Cosmochimica Acta 36, 597

Hallenbeck S.L., Nuth III J.A., Daukantas P.L., 1998, Icarus 131, 198

Hashimoto A., 1990, Nat 347, 53

John M., Sedlmayr E., 1997, Ap&SS 251, 219

Jones A.P., 1990, MNRAS 245, 331

Landolt-Börnstein, 1968, In: Schäfer K. (ed.) Zahlenwerte und Funktionen. Vol. 5b, Springer Verlag, Heidelberg

Lattimer J.M., Schramm D.N., Grossman L., 1978, ApJ 219, 230

Lenzuni P., Gail H.-P., Henning Th., 1995, ApJ 447, 848

Lide R.D., 1995, CRC Handbook of Chemistry and Physics. 76th ed., CRC Press, Boca Raton

Little-Marenin I.R., Little S.J., 1990, AJ 90, 1173

Loup C., Forveille T., Omont A., Paul J.F., 1993, A&AS 99, 291

Lucy L.B., 1971, ApJ 163, 95

Lucy L.B., 1976, ApJ 205, 482

Martin P.G., 1995, ApJ 445, L63

Mathis J.S., 1996, ApJ 472, 643

Mathis J.S., Rumpl W., Nordsieck K.H., 1977, ApJ 217, 425

Morioka M., 1981, Geochimica et Cosmochimica Acta 45, 1573

Mutschke H., Begemann B., Dorschner J, et al., 1998, A&A 333, 188

Nagahara H., Kushiro I., Mysen B.O., Moro H., 1988, Nat 331, 516

Nagahara H., Ozawa K., 1994, Meteoritics 29, 508

Nagahara H., Ozawa K., 1996, Geochimica et Cosmochimica Acta 60, 1445

Nagahara H., Kushiro I., Mysen B.O., 1994, Geochimica et Cosmochimica Acta 58, 1951

Nittler L.R., Alexander C.M.O'D., Gao X., Walker R.M., Zinner E., 1997, ApJ 483, 475

Nuth J.A., Donn B., 1982a, ApJ 257, L103

Nuth J.A., Donn B., 1982b, J. Chem. Phys. 77(5), 2639

Onaka T., de Jong T., Willems F.J., 1989, A&A 218, 169

Richtmyr R.D., Morton K.W., 1967, Difference Methods for Initial-Value Problems. Interscience Publishers, New York

Rietmeijer J.M., Nuth III J.A., MacKinnon I.D.R., 1986, Icarus 66, 211

Rybicki G.B., Hummer D.G., 1991, A&A 245, 171

Salpeter E.E., 1977, ARA&A 15, 267

Saxena S.K., Eriksson G., 1986, In: Saxena S.K. (ed.) Chemistry and Physics of Terrestrial Planets. Springer, New York, p. 30

Schaaf S.A., 1963, In: Flügge S. (ed.) Encyclopedia of Physics. Vol. VIII/2, Springer, p. 591

Sharp C.M., Huebner W.F., 1990, ApJS 72, 417

Stencel R.E., Nuth III J.A., Little Marenin I.R., Little S.J., 1990, ApJ 350, L45

Vardya M.S., de Jong T., Willems F.J., 1986, ApJ 304, L29

Waters L.B.F.M., Molster F.J., de Jong T., et al., 1996, A&A 315, L361